Dr Rémi Cardinael
CIRAD – UR AIDA
Avenue d'Agropolis
34398 Montpellier, France
+33 (0)4.67.61.56.88
Mail: remi.cardinael@cirad.fr

Dear Editor,

We acknowledge receipt of the review concerning our manuscript (bg-2017-125) entitled "**High organic inputs explain shallow and deep SOC storage in a long-term agroforestry system – Combining experimental and modeling approaches.**" by Rémi Cardinael, Bertrand Guenet, Tiphaine Chevallier, Christian Dupraz, Thomas Cozzi and Claire Chenu.

One of the reviewer was very satisfied by the corrections we made and recommended this manuscript to be published in its current form. The other reviewer however requested additional modifications.

We took most of its comments into consideration in this version. However, some of them were directly related to the optimization method we used. Our optimization method is different from the method he suggested but it is also recognized as a valid optimization method (Santaren et al., 2007, Barré et al., 2010). If it could be interesting to compare both methods as suggested by the reviewer, we consider that it is a different work. It would require a long time and a complete reorganization of the paper. Optimization procedures would have to be done again, as well as model runs and outputs' representation. Therefore, we decided not to do the requested changes concerning the optimization method. On the contrary, we better explained our method and detailed why it was valid.

Other comments were related to the grid resolution. The purpose of the work was not to provide a fully flexible model, but to have a model adapted to our data and able to answer our questions. We tried a finer grid resolution and it did not change much the results. We agreed that adding details on the resolution would dilute the main message of the paper.

From the beginning of the reviewing process, both reviewers agreed on the originality and on the impressive measured data set from the oldest agroforestry trial in Europe (18 years old): crop yields, tree growth, all fresh organic litter inputs to soil, organic carbon stocks down to 2 m depth to show that the increase of organic inputs to soil was able to explain SOC storage in these systems. These results have global interest since long-term studies on SOC sequestration are scarce, especially in temperate agroforestry systems. We showed that agroforestry systems are part of the solution to help mitigating climate change. These systems are also food producing systems (compared to afforestation for instance), and are therefore of high interest for the "4 per 1000, *Soils for food security and climate* Initiative" (http://4p1000.org/). Modeling SOC dynamics in these spatially heterogeneous systems is necessary and new.

We still think that Biogeosciences is the most appropriate journal for such a work, and we hope we were able to convince the Editor and the reviewers of the quality of this work.

Best regards,

Rémi Cardinael, on behalf of the co-authors

Montpellier, November 14th, 2017

ASSOCIATE EDITOR

I have now received two reviewer reports. While one of the reviewers is satisfied with the revision, serious concerns are expressed by the other that need further consideration. Please make carefully sure to extend and change the manuscript accordingly. Report all changes to the manuscript with clear reference to the reviewer comments they address.

Response: We took into account several points raised by the first referee, but we were not able to fully answer all of them.

NOTE for the reviewers: Pages and lines refer here to the marked-up manuscript version.

REPORT 1, REFEREE 2

I find that the revised manuscript is greatly improved. The study provides a valuable contribution to improving our understanding of soil carbon dynamics in agroforestry systems. The authors have adequately addressed all of my previous comments. I therefore recommend that this manuscript may be published in its current form.

Response: Thank you for your comments.

REPORT 2, REFEREE 1

The presentation of the manuscript improved compared to the previous version, but not enough. Some required additional analysis has not been done. With the better representation several issues became more clear that need to be tackled. The manuscript should only be published with more serious work on reacting on the review comments.

Response:

The study reports changes across the entire soil profile. However, changes seem to be most important in the top 20cm and in the tree alleys (See strange legend in Fig 4 bottom with a change in magnitude for one level). When reading only about the aggregated results, it implied to me different conclusions than reading the full paper in detail. The authors did some small notes in reacting on review requests for these details but did very little adjustments in presenting the overall results. I suggest reporting and discussing results independently in a) tree-alleys, b) top 20cm in rows c) below 20cm d) aggregated space.

Response: The reviewer is correct, most of the additional SOC storage was located in the topsoil, especially in the tree rows. We tried to reorganize the results and the discussion parts as proposed by the reviewer, not only the ones concerning SOC stocks, but also the ones concerning OC inputs:

“In the alleys of the18-year-old agroforestry system, measured organic carbon (OC) inputs from the crop residues and roots were reduced compared to the control plot due a lower crop yield (Fig. 3). This reduction in crop OC inputs was offset by OC inputs from the tree roots and tree litterfall. Total root OC inputs in the alleys (crop + tree roots) and in the control plot (crop roots) were very similar, respectively 2.43 and 2.29 t C ha^{-1} yr^{-1}. Alleys received 0.60 t C ha^{-1} yr^{-1} more of total aboveground biomass (crop residues + tree litterfall) than the control, which was added to the plough layer. Tree rows received 2.35 t C ha^{-1} yr^{-1} more C inputs in the first 0.3 m of soil compared to the control plot, mainly from the herbaceous vegetation. Down the whole soil profile, tree rows received two times more OC inputs compared to the control plot (Fig. 3), and 65% more than alleys. Overall, the agroforestry plot had 41% more OC inputs to the soil than the control plot to 2 m depth (3.80 t C ha^{-1} yr^{-1} compared to 2.69 t C ha^{-1} yr^{-1})” (P30-L646-657).

“In the first 0.3 m of soil, SOC stocks were significantly higher in the alleys than in the control plot, but the difference was small (2.1 ± 0.6 t C ha^{-1}). Between 0.3 and 1.0 m, the difference of SOC stocks was smaller but still significant. However, between 1 and 2 m depth, SOC stocks were significantly lower in the alleys than in the control. As a consequence, there was no significant difference of total SOC stocks between the two locations down the whole soil profile. In the tree rows, topsoil organic carbon stocks (0.0-0.3 m) were much higher than in the control (+ 17.0 ± 1.4 t C ha^{-1}). SOC stocks in the tree rows were also significantly higher than in the control down 1.5 m depth, but the difference was small. The opposite was observed between 1.5 and 2.0 m depth. Delta of total SOC stocks between the tree rows and the control plot was 20 ± 1.6 t C ha^{-1}. At the plot scale, total SOC stocks were significantly higher in the agroforestry plot compared to the control plot down 2 m depth (+ 3.3 ± 0.9 t C ha^{-1})” (P31-L661-671).

“In the alleys, higher SOC stocks in the topsoil could be explained by inputs from litterfall and tree roots despite a decrease in crop inputs. Most of additional SOC storage in the agroforestry plot was found in the topsoil in the tree rows. The same distribution was observed for OC inputs to the soil. Inputs from the herbaceous vegetation had an important impact on SOC storage. The increased SOC stocks in the tree rows were largely explained by an important above-ground carbon input (2.13 t C ha-1 yr-1) by the herbaceous vegetation between trees. This result had already been suggested by Cardinael et al., (2015b) and by Cardinael et al., (2017) who showed that even young agroforestry systems could store SOC in the tree rows while trees are still very small. These “grass strips” indirectly introduced by the tree planting in parallel tree rows have a major impact on SOC stocks of agroforestry systems. Increased SOC stocks below the plough layer could be explained by higher root inputs, but these inputs could also have contributed to decrease SOC stocks below 1.5 m due to priming effect. At the plot scale, measured organic carbon inputs to the soil were increased by 40% (+1.1 t C ha^{-1} yr^{-1}) down 2 m depth in the 18-year-old agroforestry plot compared to the control plot, resulting in increased SOC stocks of 3.3 t C ha^{-1}” (P40-L754-759).

The study claims performing a Bayesian analysis because it applies prior information on model parameters. However, exact prior information is still not presented (e.g. diagonal values of P_b in eq. 34) let alone motivated sufficiently. Moreover prediction uncertainty is not presented and reasons for not doing that are very weak (see detailed comments). Uncertainties and full probability distributions are essential components of a Bayesian analysis. I again require to

present and motivate the priors and to discuss predictive uncertainties. I still recommend using log-transformed parameters (and hence log-normal prior information) where prior parameter ranges span several orders of magnitude.

Response: Here we used a BFGS algorithm for some reasons detailed below. This method does not allow considering uncertainties in the prior and is sensitive to local minimum. To overcome this difficulty, we launched the optimization procedure 30 times with different set of priors and we chose the set of prior/posterior corresponding to the lowest cost function value. This approach has been used previously by Santaren et al., 2007 or Barré et al. 2010. The different set of priors were randomly chosen within the range we fixed (see table 5, page 34). Following the comment of the referee, we now presented the prior information on a log base. However, we did not perform the optimization on a log base as the f_1 and f_2 parameters were also optimized and comprised between 0 and 1.

The presentation of the numerical solution is now sufficient to be understood. There is still works to do on notation (see detailed comments). Why did the authors not check that the resolution of the spatial grid is sufficient? Why should the spatial modeling grid be regular? In the used Soetart's ode.1d code there is no such constraint. With looking at the results, I again strongly recommend repeating the analysis with a finer vertical resolution at the top 30cm.

Response: We used a regular grid because most of the information we had on the boundaries' conditions were at a regular vertical resolution of 10 cm or 20 cm (root biomass, clay, bulk density, etc.) as well as the data we had to evaluate the model. We run the model with 5 cm resolution and compared it with our original version of 10 cm (see the Figure 1 below presenting the SOC profiles in kg m^{-3} for both resolutions). The results are slightly different mainly because of the thresholds we fixed to define the inputs. For instance, we assume that the aboveground litter goes entirely into the first soil layer. Thus, the concentration in the first layer is higher for finer resolution inducing different diffusive fluxes. We do not fully understand what would be the interest of changing the vertical resolution. The model was not designed to be fully flexible in terms of vertical resolution and it would need an important rewriting of the model. Since the resolution we used correspond to the resolution of the data and it gives good fits we considered that our model outputs are robust enough.

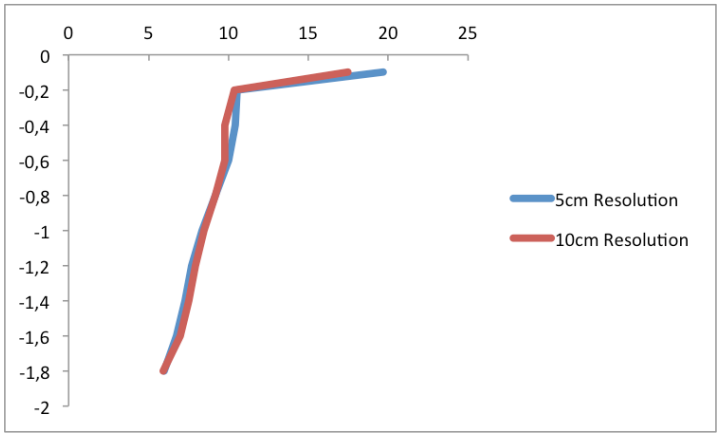

Figure 1. Modeled SOC content (kg m^{-3}) with the two pools' model without priming effect with two grid resolutions.

I can see the point in the current quantifying the priming effect with transferring the decomposition of the priming model to the agroforestry plot with a parameter fixed to conditions of the control (L 627ff). However, I do not agree in the interpretation. To me it is not an absence of priming but is the priming effect as it worked in the control. I still have difficulties in accepting the approach. For me it does not make sense to apply the priming-explicit model with parameter fixed to the control as a no-priming base scenario. Also the results of this run with stock increases of 60t/ha in 18 years are not reasonable (Fig. 6). I am still curious on the comparison of the current quantification to the (to my opinion more straightforward and without much work obtainable) model comparisons I suggested in the previous review involving comparison of priming-explicit vs. no-priming model variants. Therefore, I cannot follow the numbers in abstract of priming effects reducing potential SOC storage by 75 to 90%. (In addition one should differentiate between tree rows/alleys and different depth)

Response: We agree with the reviewer, the reference in the control plot does not correspond to an absence of priming, but to the priming effect as it worked in the control, i.e. induced by the annual crop inputs. This was not clearly stated in the manuscript. However, we were here interested in quantifying the additional priming effect induced by the trees and the tree row vegetation. Applying the priming explicit model with parameter fixed to the control was necessary to have a baseline in the agroforestry plot of the priming effect induced by the crops. It is not possible to quantify the priming effect intensity by just comparing priming-explicit vs. no-priming model variant, because the decomposition rate of the no-priming effect variant implicitly takes priming into account: as a consequence, total modeled SOC stocks were slightly higher with the priming-explicit model variant than with the no-priming model variant (116.68 tC/ha vs 116.28 tC/ha in the tree rows, 105.34 tC/ha vs 106.27 tC/ha in the alleys).

But we agree with the reviewer that this methodology and its interpretation in hard to grasp, and this will probably be the case for future readers. As this part is not central in our study, we decided to remove all this paragraph concerning the estimation of the priming intensity, in the Materials and Methods (P29-30-L612-642) and in the results (P39-L40-L734-749). Figure 6 and figure S3 were then removed. It also has the advantage to reduce the manuscript length.

Detailed comments

Table 5 caption: "the prior values that minimized J(x)". Why is the prior information different for different model variants? I hope that you did not try/optimize for different prior information means. Prior information is defined as an information that is independent of the observations and the calibration. Please add an additional column with mean and standard deviation of the prior parameter pdf.

Response: Here, we used a classical gradient method for reasons that were not clearly explained in the manuscript. We have used a variational scheme to minimize a cost function based on the calculation of the gradient of the cost function with respect to the parameter assuming that all uncertainties are Gaussian (Tarantola, 1987). This is a strong assumption that greatly simplifies the calculation and characterization of the solution.

- First, we should mention that this study is a part of a bigger project aiming to represent the

soil C profile in the global land surface model ORCHIDEE (Krinner et al., 2005) with different plant functional type on the same grid. A study case with an agroforestry plot was ideal to test the structure of the model. One objective is to be able to optimize the vertically-discretized soil carbon model embedded in ORCHIDEE using various data streams. In a first step, we decided to start with a simple model, isolated from ORCHIDEE, to be able to run several test without the computing needs of a land surface model. The second step will be to use the whole model and to optimize with a variational approach all parameters of ORCHIDEE. The choice of a variational approach versus a monte carlo one follows from running time constrain that may be prohibitive with a monte carlo approach and a complex process-based model.

- Following that point, we need to recall that we have already performed several parameter optimization studies with the ORCHIDEE model using the same variational approach (Santaren et al 2007, Verbeeck et al. 2011, Kuppel et al. 2012) and that through these studies we gained confidence that the level of non linearities considered in the proposed soil carbon models do not prevent the variational algorithm to obtain a satisfactory solution, provided few cautions. The only requirements or cautions are the need to perform several optimization starting from different prior parameter values, randomly distributed in their allowed range of variation. We then select the case that provides the lowest cost function. With this approach we are much less sensitive to potential local minima. This explain why we have different prior values.

Fig. 4. I is still interesting to compare depth profiles across control, tree row, and alley. I agree that the closeness of the values makes a combined plot hard to read. But it is even harder to compare across facets. Please, make an attempt to display at least the data or one variant of the prediction in one plot.

Response: We made the following plot to compare depth profiles across control, tree row and alley:

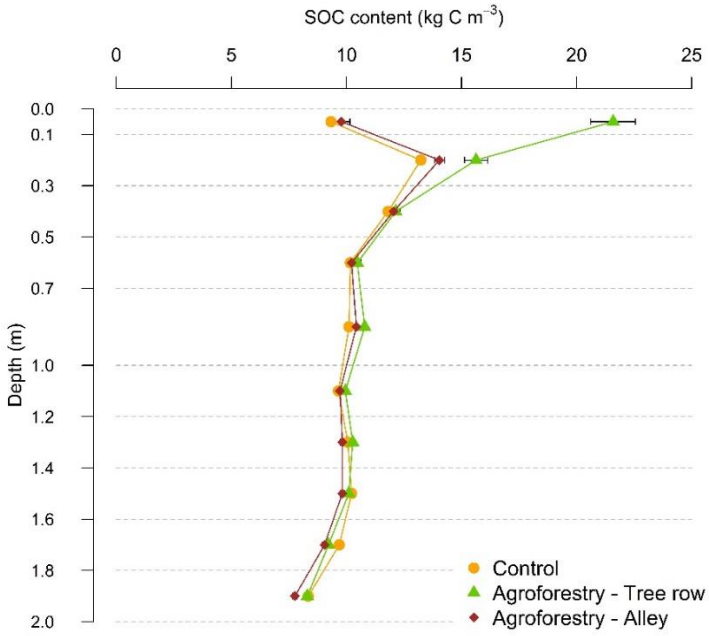

Figure 2. Measured SOC content in the 18-year-old agroforestry system.

As these data were already published in Cardinael et al. (2015) (*Geoderma*), it was not added to the manuscript that already contains many graphs. It could be done if the reviewer thinks it is necessary.

Fig 5. First I though the [10,11] entry in legend of the bottom subplot was an error of omitting the decimal point, but the change of magnitude and the non-continuous scale are deliberate. Please, make this really obvious and discuss.

Response: Two parallel oblique line were added on the graph to symbolize the change in magnitude in the scale. We also added the following sentence in the legend: "The scale used in the middle and bottom panels are not continuous due to the large stocks predicted by the model in the top layer in the tree-row." (P38-L731-733). It is also discussed P39-L758-764 and P42-43-L820-823.

Eq 12 (and other eq.): Notations (here d for \partial) dFoc/dt and dFoc_t,z,d/dt are ambiguous. Eq. 14 for dFoc/dt involves terms specific to t,z,d. I suggest renaming all dFoc/dt to dFoc_t,z,d/dt and renaming all previous dFoc_t,z,d/dt to dec_Foc_t,z,d as it only describes decomposition/mineralization. Similar for HSOC.

Response: We agree these equations were ambiguous, we therefore modified them as requested by the reviewer (P12-L261; P14-L295-296; P14-L302-303; P17-L358-372).

L 649: Suggest modifying "importance of of priming" to "importance of additional priming due to tree row vegetation and trees"

Response: This sentence and this paragraph were removed (see above)

L 654: I do not agree with "correspond to the absence of priming due to trees". To my opinion it corresponds to "same magnitude of the priming effect as in the control". See may general comments on my difficulties with the current priming effect quantification.

Response: This sentence and this paragraph were removed (see above)

L 567: Please write more specifically what is "the associated uncertainty". In the previous sentence the known is "These parameters". The 93 soil samples estimate the uncertainty of observed C stocks. How did you use the uncertainty of the observed stocks in the optimization?

Response: Since we used a classical gradient method, the BFGS method needs as input the variance of the observation. We therefore associated a variance matrix read by the algorithm.

L 605: Manzoni et al 2012 is not a good citation for BIC. Please go back to the original literature cited therein.

Response: This reference has been deleted, and was replaced by Schwarz, 1978 (P28-L596-599).

Eq. 21: I still do not understand the reasons for using an unusual variant of BIC when you

defined your Likelihood by the first term in eq. 21. In effect the current BIC variant uses some different Likelihood that ignores observation uncertainty used in matrix R in eq. 21. It might be an adequate Likelihood for the Manzoni 2012 studied system, but I cannot see how it applies to your case. It would have been very easy to report the requested standard BIC formulation alongside your variant.

Response: We changed the BIC variant to come back to the standard BIC formulation using the likelihood (P28-L596-599). Absolute values have changed, but relative values did not (results are the same for the model comparison) (P37, Fig. 4).

L 836: Why do the correlations hinder you to compute prediction uncertainty? They are important to consider in Bayesian analysis. The straightforward way would be an MCMC run on eq. 21 to obtain a proper sample from posterior parameter distribution. Perhaps more easy: From the curvature at the optimum you already got and report correlations of a first approximation of a multivariate normal of the parameters posterior distribution. You can draw samples from this distribution and do (say ~1000) forward model runs to compute 95% confidence interval on predictions.

Response: As explained in one of the answer above, we used a BFGS algorithm which is as efficient as a MCMC to reduce the cost function if enough set of parameters are used to launch the algorithm. In our case, we used 30 different sets of priors to avoid local minima, we do believe that the cost function was well minimized as suggested by the Figure 3 below where the cost function reached a limit after the use of 15 set of priors.

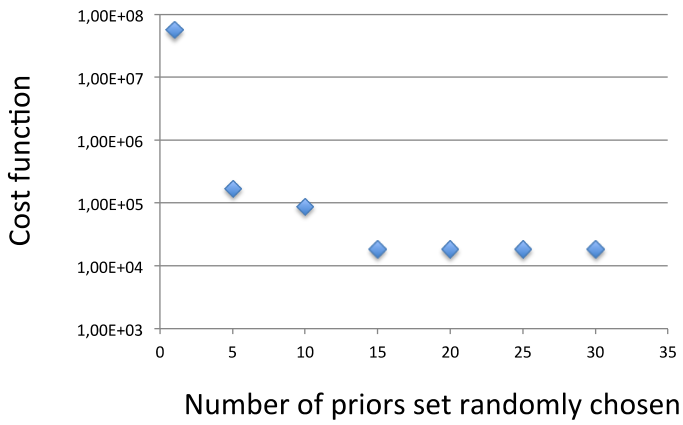

Figure 3. Value of the cost function related to the number of prior sets.

L 902ff: I suggest moving the part on differences in soil temperature and soil moisture and the sensitivity study to the part where you describe what you have not done "simplifying assumptions". Instead of strongly concluding that OC inputs drive SOC storage I recommend formulating more weakly that in this study OC inputs are sufficient to explain the differences in stocks. (You did not compare to explicitly modelling the differences in temperature and moisture with the agroforestry)

Response: The part on differences in soil temperature and soil moisture as well as the sensitivity study was moved above, in the simplifying assumptions (P41-L774-786). We also

softened our conclusion as suggested by the reviewer: “This strong validation also revealed that OC inputs were sufficient to explain the differences in SOC stocks at this site.” (P41-L789-790).

L 996: Its a result section. “results were not significantly different” ? Hence, ...

Response: It was changed to then “Hence, we considered that changes in litter quality in the agroforestry plot did not significantly influence SOC decomposition rates.” (P45-L884-885).

High organic inputs explain shallow and deep SOC storage in a long-term agroforestry system – Combining experimental and modeling approaches.

Rémi Cardinael[a,b,c,d]*, Bertrand ~~Guenet~~[d]Guenet[e], Tiphaine Chevallier[a], Christian ~~Dupraz~~[e]Dupraz[f], Thomas Cozzi[b], Claire Chenu[b]

[a] Eco&Sols, IRD, CIRAD, INRA, Montpellier SupAgro, Univ Montpellier, Montpellier, France~~IRD, UMR Eco&Sols, Montpellier SupAgro, 2 place Viala, 34060 Montpellier, France~~

[b] AgroParisTech, UMR Ecosys, Avenue Lucien Brétignières, 78850 Thiverval-Grignon, France

[c] CIRAD, UPR AIDA, ~~Avenue d'Agropolis,~~F-34398 Montpellier, France (present address)

[d] AIDA, Univ Montpellier, CIRAD, Montpellier, France

~~[d-e]~~Laboratoire des Sciences du Climat et de l'Environnement, UMR CEA-CNRS-UVSQ, CE L'Orme des Merisiers, 91191 Gif-Sur-Yvette, France

~~[e-f]INRA, UMR~~ System, INRA, CIRAD, Montpellier SupAgro, ~~2 place Viala, 34060~~Univ Montpellier, Montpellier, France

* Corresponding author. Tel.: +33 04.67.61.53.08. E-mail address: remi.cardinael@cirad.fr

Keywords: priming effect, deep roots, deep soil organic carbon, spatial heterogeneity, silvoarable system, crop yield, SOC modeling

Abstract

Agroforestry is an increasingly popular farming system enabling agricultural diversification and providing several ecosystem services. In agroforestry systems, soil organic carbon (SOC) stocks are generally increased, but it is difficult to disentangle the different factors responsible for this storage. Organic carbon (OC) inputs to the soil may be larger, but SOC decomposition

rates may be modified owing to microclimate, physical protection, or priming effect from roots, especially at depth. We used an 18-year-old silvoarable system associating hybrid walnut trees (*Juglans regia* × *nigra*) and durum wheat (*Triticum turgidum* L. subsp. *durum*), and an adjacent agricultural control plot to quantify all OC inputs to the soil - leaf litter, tree fine root senescence, crop residues, and tree row herbaceous vegetation -, and measure SOC stocks down 2 m depth at varying distances from the trees. We then proposed a model that simulates SOC dynamics in agroforestry accounting for both the whole soil profile and the lateral spatial heterogeneity. The model was calibrated to the control plot only.

Measured OC inputs to soil were increased by about 40% (+ 1.11 t C ha^{-1} yr^{-1}) down to 2 m depth in the agroforestry plot compared to the control, resulting in an additional SOC stock of 6.3 t C ha^{-1} down to 1 m depth. The model was strongly validated, describing properly the measured SOC stocks and distribution with depth in agroforestry tree rows and alleys. It showed that the increased inputs of fresh biomass to soil explained the observed additional SOC storage in the agroforestry plot. Moreover, only a priming effect variant of the model was able to capture the depth distribution of SOC stocks. ~~Modeling revealed a strong priming effect that would reduce the potential SOC storage due to higher organic inputs in the agroforestry system by 75 to 90%.~~ This result questions the potential of soils to store large amounts of carbon, especially at depth. Deep-rooted trees modify OC inputs to soil, a process that deserves further studies given its potential effects on SOC dynamics.

1 Introduction

Agroforestry systems are complex agroecosystems combining trees and crops or pastures within the same field (Nair, 1993, 1985; Somarriba, 1992). More precisely, silvoarable systems associate parallel tree rows with annual crops. Some studies showed that these systems could be very productive, with a land equivalent ratio (Mead and Willey, 1980) reaching up to 1.3

(Graves et al., 2007). Silvoarable systems may therefore produce up to 30% more marketable biomass on the same area of land compared to crops and trees grown separately. This performance can be explained by a better use of water, nutrients and light by the agroecosystem throughout the year. Trees grown in silvoarable systems usually grow faster than the same trees grown in forest ecosystems, because of their lower density, and because they also benefit from the crop fertilization (Balandier and Dupraz, 1999; Chaudhry et al., 2003; Chifflot et al., 2006). In temperate regions, farmers usually grow one crop per year, and this association of trees can extend the growing period at the field scale, especially when winter crops are intercropped with trees having a late bud break (Burgess et al., 2004). However, after several years, a decrease of crop yield can be observed in mature and highly dense plantations, especially close to the trees, due to competition between crops and trees for light, water, and nutrients (Burgess et al., 2004; Dufour et al., 2013; Yin and He, 1997).

Part of the additional biomass produced in agroforestry is used for economical purposes, such as timber or fruit production. Leaves, tree fine roots, pruning residues and the herbaceous vegetation growing in the tree rows will usually return to the soil, contributing to a higher input of organic carbon (OC) to the soil compared to an agricultural field (Peichl et al., 2006).

In such systems, the observed soil organic carbon (SOC) stocks are also generally higher compared to a cropland (Albrecht and Kandji, 2003; Kim et al., 2016; Lorenz and Lal, 2014). Cardinael *et al.*, (2017) measured a mean SOC stock accumulation rate of 0.24 (0.09-0.46) t C ha^{-1} yr^{-1} at 0-30 cm depth in several silvoarable systems compared to agricultural plots in France. Higher SOC stocks were also found in Canadian agroforestry systems, but measured only to 20 cm depth (Bambrick et al., 2010; Oelbermann et al., 2004; Peichl et al., 2006).

To our knowledge, we are still not able to disentangle the factors responsible for such a higher SOC storage. This SOC storage might be due to higher OC inputs but it could also be favored

by a modification of the SOC decomposition owing to a change in SOC physical protection (Haile et al., 2010), and/or in soil temperature and moisture.

The introduction of trees in an agricultural field modifies the amount, but also the distribution of fresh organic carbon (FOC) input to the soil, both vertically and horizontally (Bambrick et al., 2010; Howlett et al., 2011; Peichl et al., 2006). FOC inputs from the trees decrease with increasing distance from the trunk and with soil depth (Moreno et al., 2005). On the contrary, crop yield usually increases with increasing distance from the trees (Dufour et al., 2013; Li et al., 2008). Therefore, the proportions of FOC coming from both the crop residues and the trees change with distance from the trees, soil depth, and time.

Tree fine roots (diameter ≤ 2 mm) are the most active part of root systems (Eissenstat and Yanai, 1997) and play a major role in carbon cycling. In silvoarable systems, tree fine root distribution within the soil profile is strongly modified due to the competition with the crop, inducing a deeper rooting compared to trees grown in forest ecosystems (Cardinael et al., 2015a; Mulia and Dupraz, 2006). Deep soil layers may therefore receive significant OC inputs from fine root mortality and exudates. Root carbon has a higher mean residence time in the soil compared to shoot carbon (Kätterer et al., 2011; Rasse et al., 2006), presumably because root residues are preferentially stabilized within microaggregates or adsorbed to clay particles. Moreover, temperature and moisture conditions are more buffered in the subsoil than in the topsoil. The microbial biomass is also smaller at depth (Eilers et al., 2012; Fierer et al., 2003), and the spatial segregation with organic matter is larger (Salomé et al., 2010) resulting in lower decomposition rates. Deep root carbon input in the soil could therefore contribute to a SOC storage with high mean residence times. However, some studies showed that adding FOC – a source of energy for microorganisms - to the subsoil enhanced decomposition of stabilized carbon, a process called « priming effect » (Fontaine et al., 2007). The priming effect is stronger when induced by labile molecules like root exudates than by root litter coming from the decomposition of

dead roots (Shahzad et al., 2015). Therefore, the net effect of deep roots on SOC stocks has to be assessed, especially in silvoarable systems.

Models are crucial as they allow virtual experiments to best design and understand complex processes in these systems (Luedeling et al., 2016). Several models have been developed to simulate interactions for light, water and nutrients between trees and crops (Charbonnier et al., 2013; Duursma and Medlyn, 2012; van Noordwijk and Lusiana, 1999; Talbot, 2011) or to predict tree growth and crop yield in agroforestry systems (Graves et al., 2010; van der Werf et al., 2007). However, none of these models are designed to simulate SOC dynamics in agroforestry systems and they are therefore not useful to estimate SOC storage. Oelbermann & Voroney (2011) evaluated the ability of the CENTURY model (Parton et al., 1987) to predict SOC stocks in tropical and temperate agroforestry systems, but with a single-layer modeling approach (0-20 cm). The approach of modeling a single topsoil layer assumes that deep SOC does not play an active role in carbon cycling, while it was shown that deep soil layers contain important amounts of SOC (Jobbagy and Jackson, 2000), and that part of this deep SOC could cycle on decadal timescales due to root inputs or to dissolved organic carbon transport (Baisden and Parfitt, 2007; Koarashi et al., 2012). The need to take into account deep soil layers when modeling SOC dynamics is now well recognized in the scientific community (Baisden et al., 2002; Elzein and Balesdent, 1995), and several models have been proposed (Braakhekke et al., 2011; Guenet et al., 2013; Koven et al., 2013; Taghizadeh-Toosi et al., 2014; Ahrens et al., 2015). Using vertically discretized soils is particularly important when modeling the impact of agroforestry systems on SOC stocks, but to our knowledge, vertically spatialized SOC models have not yet been tested for these systems.

The aims of this study were then twofold: (i) to propose a model of soil C dynamics in agroforestry systems able to account for both vertical and lateral spatial heterogeneities and (ii)

to test whether variations of fresh organic carbon (FOC) input could explain increased SOC stocks both using experimental data and model runs.

For this, we first compiled data on FOC inputs to the soil obtained in a 18-year-old agroforestry plot and in an agricultural control plot in southern France, in which SOC stocks have been recently quantified to 2 m depth (Cardinael et al., 2015b). FOC inputs comprised tree fine roots, tree leaf litter, aboveground and belowground biomass of the crop and of the herbaceous vegetation in the tree rows. We compiled recently published data for FOC inputs (Cardinael et al., 2015a; Germon et al., 2016), and measured the others (Table 1).

We then modified a two pools model proposed by Guenet *et al.*, (2013), to create a spatialized model over depth and distance from the tree, the CARBOSAF model (soil organic CARBOn dynamics in Silvoarable AgroForestry systems). Based on data acquired since the tree planting in 1995 (crop yield, tree growth), and on FOC inputs, we modeled SOC dynamics to 2 m depth in both the silvoarable and agricultural control plot. We evaluated the model against measured SOC stocks along the profile and used this opportunity to test the importance of priming effect (*PE*) for deep soil C dynamics in a silvoarable system. The performance of the two pools model including *PE* was also compared with a model version including three OC pools.

2 Materials and methods

2.1 Study site

The experimental site is located at the Restinclières farm Estate in Prades-le-Lez, 15 km North of Montpellier, France (longitude 04°01’ E, latitude 43°43’ N, elevation 54 m a.s.l.). The climate is sub-humid Mediterranean with an average temperature of 15.4°C and an average annual rainfall of 973 mm (years 1995–2013). The soil is a silty and carbonated (pH = 8.2) deep alluvial Fluvisol (IUSS Working Group WRB, 2007). In February 1995, a 4.6 hectare

150 silvoarable agroforestry plot was established with the planting of hybrid walnut trees (*Juglans*
151 *regia* × *nigra* cv. NG23) at a density of 192 trees ha^{-1} but later thinned to 110 trees ha^{-1}. Trees
152 were planted at 13 m × 4 m spacing, and tree rows are East–West oriented. The cultivated alleys
153 are 11 m wide. The remaining part of the plot (1.4 ha) was kept as an agricultural control plot.
154 Since the tree planting, the agroforestry alleys and the control plot were managed in the same
155 way. The associated crop is most of the time durum wheat (*Triticum turgidum* L. subsp. *durum*),
156 except in 1998, 2001 and 2006, when rapeseed (*Brassica napus* L.) was cultivated, and in 2010
157 and 2013, when pea (*Pisum sativum* L.) was cultivated. The soil is ploughed to a depth of 0.2
158 m before sowing, and the wheat crop is fertilized with an average of 120 kg N ha^{-1} yr^{-1}. Crop
159 residues (wheat straw) are also exported, but about 25% remain on the soil. Tree rows are
160 covered by spontaneous herbaceous vegetation. Two successive herbaceous vegetation types
161 occur during the year, one in summer and one in winter. The summer vegetation is mainly
162 composed of *Avena fatua* L., and is 1.5 m tall. In winter, the vegetation is a mix of *Achillea*
163 *millefolium* L., *Galium aparine* L., *Vicia* L., *Ornithogalum umbellatum* L. and *Avena fatua* L,
164 and is 0.2 m tall.
165
166 **Table 1.** Synthesis of the different field and laboratory data available or measured, and their
167 sources.

Description of the data	Source
Soil texture, bulk densities, SOC stocks	Cardinael *et al.*, (2015a)
Soil temperature and soil moisture	Measured
Tree growth (DBH)	Measured
Tree wood density	(Talbot, 2011)
Tree fine root biomass	Cardinael *et al.*, (2015b)
Tree fine root turnover	Germon *et al.*, (2016)
Crop yield and crop ABG biomass	Dufour *et al.*, (2013) and measured
Crop root biomass	Prieto *et al.*, (2015) and measured
Tree row herbaceous vegetation – ABG biomass	Measured
Tree row herbaceous vegetation – root biomass	Measured
Biomass carbon concentrations	Measured
Potential decomposition rate of roots	Prieto *et al.*, (2016a)
HSOC potential decomposition rate	Measured

DBH: Diameter at Breast Height; ABG: aboveground; OC: organic carbon; HSOC: humified soil organic carbon.

2.2 Organic carbon stocks

2.2.1 Soil organic carbon stocks

SOC data have been published in Cardinael *et al.*, (2015b). Briefly, soil cores were sampled down to 2 m depth in May 2013, 100 in the agroforestry plot, and 93 in the agricultural control plot. SOC concentrations, soil bulk densities, SOC stocks, and soil texture were measured for ten soil layers (0.0-0.1, 0.1-0.3, 0.3-0.5, 0.5-0.7, 0.7-1.0, 1.0-1.2, 1.2-1.4, 1.4-1.6, 1.6-1.8, and 1.8-2.0 m). In the agroforestry plot, 40 soil cores were taken in the tree rows, while 60 were sampled in the alleys at varying distances from the trees. Soil organic carbon stocks were quantified on an equivalent soil mass basis (Ellert and Bettany, 1995).

2.2.2 Tree aboveground and stump carbon stocks

Three hybrid walnuts were chopped down in 2012. The trunk circumference was measured every meter up to the maximum height of the tree to estimate its volume. The trunk biomass was estimated by multiplying the trunk volume by the wood density that was measured at 616 kg m^{-3} during a previous work at the same site (Talbot, 2011). Then, branches were cut, the stump was uprooted, and they were weighted separately. Samples were brought to the laboratory to determine the moisture content, which enabled calculation of the branches and the stump dry mass.

2.3 Measurements of organic carbon inputs in the field

2.3.1 Carbon inputs from tree fine root mortality

192 The tree fine root (diameter ≤ 2 mm) biomass was quantified and coupled with an estimate of
193 the tree fine root turnover in order to predict the carbon input to the soil from the tree fine root
194 mortality. A detailed description of the methods used to estimate the tree fine root biomass can
195 be found in Cardinael *et al.*, (2015a). In March 2012, a 5 (length) × 1.5 (width) × 4 m (depth)
196 pit was open in the agroforestry plot, perpendicular to the tree row, at the North of the trees.
197 The tree fine root distribution was mapped down 4 m depth, and the tree fine root biomass was
198 quantified in the tree row and in the alley. Only results concerning the first two meters of soil,
199 among those obtained by Cardinael *et al.*, (2015a) will be used here.
200 In July 2012, sixteen minirhizotrons were installed in the agroforestry pit, at 0, 1, 2.5 and 4 m
201 depth, and at two and five meters from the trees. The tree root growth and mortality was
202 monitored during one year using a scanner (CI-600 Root Growth Monitoring System, CID,
203 USA), and analyzed using the WinRHIZO Tron software (Régent, Canada). A detailed
204 description of the methods and of results used to estimate the tree fine root turnover can be
205 found in Germon *et al.*, (2016).
206
207 **2.3.2 Tree litterfall**
208 In 2009, the crowns of two walnut trees were packed with a net in order to collect the leaf
209 biomass from September to January. The same was done in 2012 with three other walnut trees.
210 The leaf litter was then dried, weighted and analyzed for C to quantify the leaf carbon input per
211 tree.
212
213 **2.3.3 Aboveground and belowground input from the crop**
214 Since the tree planting in 1995, the crop yield was measured 14 times (in 1995, 2000, 2002,
215 2003, 2004, 2005, 2007, 2008, 2009, 2010, 2011, 2012, 2013, and 2014), while the wheat straw
216 biomass and the total aboveground biomass were measured six times (in 2007, 2008, 2009,

2011, 2012, and 2014) in both the control and the agroforestry plot (Dufour et al., 2013), using sampling subplots of 1 m^2 each. In the control plot, five subplots have been sampled while in the agroforestry plot five transects have been sampled. Each transect was made of three subplots, 2 m North from the tree, 2 m South from the tree, and 6.5 m from the tree (middle of the alley). In March 2012, a 2 m deep pit was opened in the agricultural control plot (Prieto et al., 2015), and the root biomass was quantified to the maximum rooting depth (1.5 m). The root:shoot ratio of durum wheat was measured in the control plot. We assumed that the crop root biomass turns out once a year, after the crop harvest.

2.3.4 Above and belowground input from the tree row herbaceous vegetation

As two types of herbaceous vegetation grow in the tree rows during the year, samples were taken in summer and winter. In late June 2014, twelve subplots of 1 m^2 each were positioned in the tree rows, around 4 walnut trees. In January 2015, six subplots of 1 m^2 each were positioned in the tree rows, around 2 walnut trees. The middle of each subplot was located at 1 m, 2 m and 3 m, respectively, from the selected walnut tree. All the aboveground vegetation was collected in each square. In the middle of each subplot, root biomass was sampled with a cylindrical soil corer (inner diameter of 8 cm). Soil was taken at three soil layers, 0.0-0.1, 0.1-0.3 and 0.3-0.5 m. In the laboratory, soil was gently washed with water through a 2 mm mesh sieve, and roots were collected. Roots from the herbaceous vegetation were easily separated manually from walnut roots, as they were soft and yellow compared to walnuts roots that were black. After being sorted out from the soil and cleaned, the root biomass was dried at 40°C and measured.

2.4 Carbon concentration measurements

All organic carbon measurements were performed with a CHN elemental analyzer (Carlo Erba NA 2000, Milan, Italy), after samples were oven-dried at 40°C for 48 hours (Table 2). Dry biomasses (t DM ha^{-1}) of each organic matter inputs were multiplied by their respective organic carbon concentrations (mg C g^{-1}) to calculate organic carbon stocks (t C ha^{-1}).

Table 2. Organic carbon concentrations and C:N ratio of the different types of biomass.

Type of biomass	Organic C concentration (mg C g^{-1})	C:N	Number of replicates
Walnut trunk	445.7 ± 1.0	159.1 ± 25.2	3
Walnut branches	428.6 ± 1.7	62.2 ± 11.7	3
Wheat straw	433.2 ± 0.7	55.5 ± 2.1	5
Wheat root	351.4 ± 19	24.8 ± 2.1	8
Walnut leaf	449.4 ± 3.7	49.1 ± 0.4	3
Walnut fine root	437.0 ± 3.3	28.6 ± 3.4	8
Summer vegetation (ABG)	448.4 ± 1.9	37.8 ± 2.2	5
Summer vegetation (roots)	314.5 ± 8.3	33.8 ± 1.7	6
Winter vegetation (ABG)	447.7 ± 5.3	11.2 ± 0.4	3
Winter vegetation (roots)	397.4 ± 5.0	24.7 ± 0.7	3

The organic matter called "vegetation" stands for the herbaceous vegetation that grows in the tree row. ABG: aboveground. Errors represent standard errors.

2.5 General description of the CARBOSAF model

2.5.1 Organic carbon decomposition

We adapted a model developed by Guenet et al. (2013) where total SOC is split in two pools, the FOC and the humified soil organic carbon (HSOC) for each soil layer (Fig. 1a). Input to the FOC pool comes from the plant litter and the distribution of this input within the profile is assumed to depend upon depth from the surface (z), distance from the tree (d), and time (t). Equations describing inputs to the FOC pool ($I_{t,z,d}$) at a given time, depth, and distance are fully explained in the Results.

The FOC mineralisation is assumed to be governed by first order kinetics, being proportional to the FOC pool, as given by:

$$\frac{\partial FOC_{t,z,d}}{\partial t} dec\_FOC_{t,z,d} = -k_{FOC} \times FOC_{t,z,d} \times f_{clay,z} \times f_{moist,z} \times f_{temp,z} \quad (1)$$

where $FOC_{t,z,d}$ is the FOC carbon pool (kg C m^{-2}) at a given time (t, in years), depth (z, in m) and distance (d, in m), and k_{FOC} is its decomposition rate. The potential decomposition rates of the different plant materials were assessed with a 16-week incubation experiment during a companion study at the site (Prieto et al., 2016). The decomposition rate k_{FOC} was weighted by the respective contribution of each type of plant litter as a function of the tree age, soil depth and distance from the tree. The rate modifiers $f_{clay,z}$, $f_{moist,z}$ and $f_{temp,z}$ are functions depending respectively on the clay content, soil moisture and soil temperature at a given depth z, and range between 0 and 1.

The f_{clay} function originated from the CENTURY model (Parton et al., 1987):

$$f_{clay,z} = 1 - 0.75 \times Clay_z \quad (2)$$

where $Clay_z$ is the clay fraction (ranging between 0 and 1) of the soil at a given depth z.

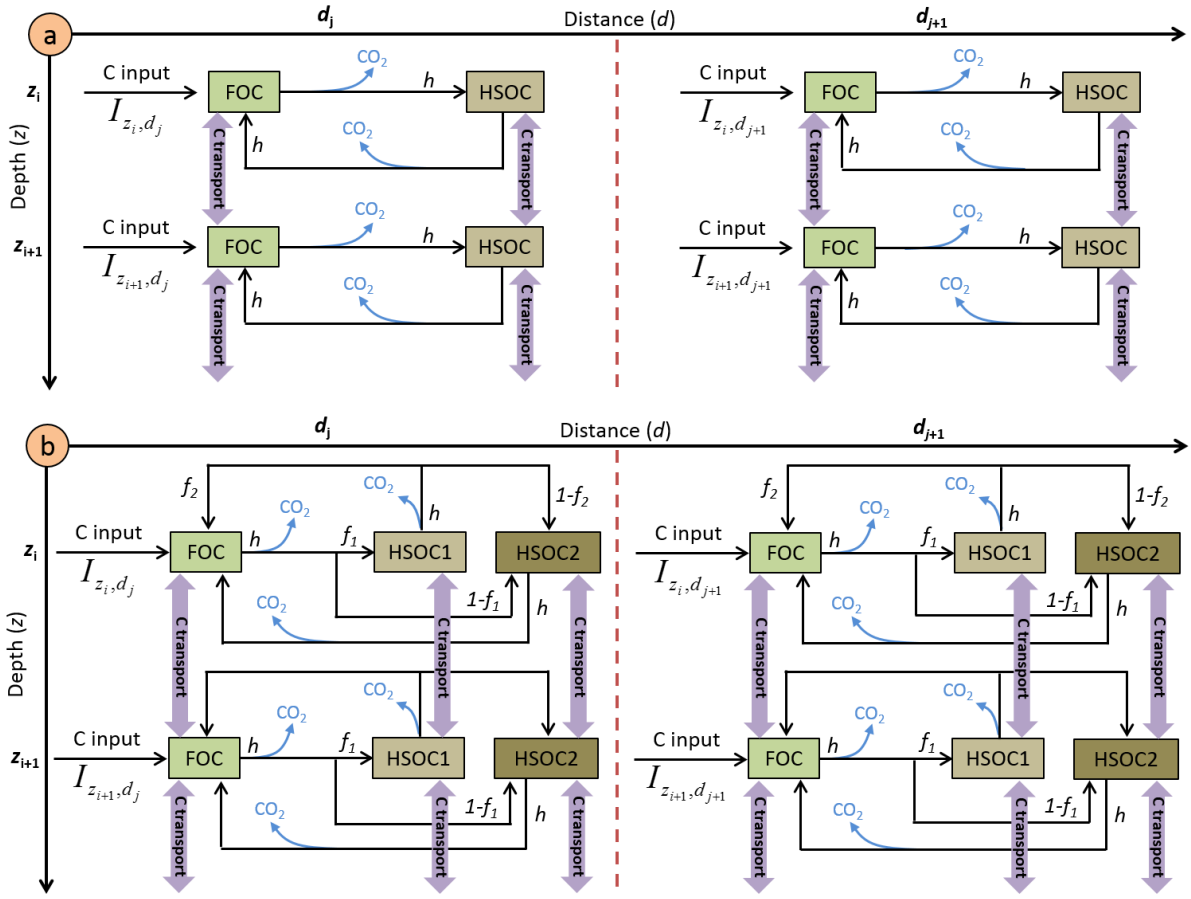

Fig. 1. Schematic representation of the pools and the fluxes of the (a) two pools model and (b) three pools model.

The $f_{moist,z}$ function originated from the meta-analysis of Moyano *et al.*, (2012) and is affected by soil properties (clay content, SOC content). Briefly, the authors fitted linear models on 310 soil incubations to describe the effect of soil moisture on decomposition. Then, they normalized such linear models between 0 and 1 to apply these functions to classical first order kinetics. All details are described in Moyano *et al.*, (2012). To save computing time, we calculated $f_{moist,z}$ only once using measured SOC stocks instead of using modelled SOC stocks and repeated the calculation at each time step.

The temperature sensitivity of the soil respiration is expressed as Q_{10}:

$$f_{temp,z} = Q_{10}^{\frac{temp_z - temp_{opt}}{10}} \quad (3)$$

with $temp_z$ being the soil temperature in K at each soil depth z and $temp_{opt}$ a parameter fixed to 304.15 K. The Q_{10} value was fixed to 2, a classical value used in models (Davidson and Janssens, 2006).

Once the FOC is decomposed, a fraction is humified (h) and another is respired as CO_2 ($1-h$) (Fig. 1a) following equations (4) and (5).

$$Humified\ FOC_{t,z,d} = h \times dec\_FOC_{t,z,d} \frac{\partial FOC_{t,z,d}}{\partial t} \quad (4)$$

$$Respired\ FOC_{t,z,d} = (1-h) \times dec\_FOC_{t,z,d} \frac{\partial FOC_{t,z,d}}{\partial t} \quad (5)$$

Two mathematical approaches are available in the model to describe the mineralisation of HSOC: a first order kinetics, as given by Eq. (6) or an approach developed by Wutzler & Reichstein, (2008) and by Guenet *et al.*, (2013) introducing the priming effect, i.e., the mineralisation of HSOC depends on FOC availability, and given by Eq. (7):

$$\frac{\partial HSOC_{t,z,d}}{\partial t} dec\_HSOC_{t,z,d} = -k_{HSOC,z} \times HSOC_{t,z,d} \times f_{moist,z} \times f_{temp,z} \quad (6)$$

$$\frac{\partial HSOC_{t,z,d}}{\partial t} dec\_HSOC_{t,z,d} = -k_{HSOC,z} \times HSOC_{t,z,d} \times (1 - e^{-PE \times FOC_{t,z,d}}) \times f_{moist,z} \times f_{temp,z} \quad (7)$$

where $HSOC_{t,z,d}$ is the humified SOC carbon pool at a given time (t, in years), depth (z, in m) and distance (d, in m), $k_{HSOC,z}$ is its decomposition rate (yr^{-1}) at a given depth z, and PE is the priming effect parameter. The parameters $f_{moist,z}$ and $f_{temp,z}$ are functions depending respectively on soil moisture and soil temperature at a given depth z, and affecting the decomposition rate of HSOC. They correspond to the moisture equation from Moyano *et al.*, (2012) and to Eq. (3),

311 respectively. The decomposition rate $k_{HSOC,z}$ was an exponential law depending on soil depth
312 (z) as shown by an incubation study (see paragraph *HSOC decomposition rate* further in the
313 M&M):

314 $$k_{HSOC,z} = a \times e^{-b \times z} \qquad (8)$$

315 The b parameter of this equation represented the ratio of labile C/stable C within the HSOC
316 pool. The effect of clay on HSOC decomposition was implicitly taken into account in this
317 equation as clay content increased with soil depth.
318 A fraction of decomposed HSOC returns to the FOC assuming that part of the HSOC
319 decomposition products is as labile as FOC (h) and another is respired as CO_2 (Fig. 1a) in the
320 two pools model.
321
322 Finally, we also developed an alternative version of the model with three pools by splitting the
323 HSOC pools into two pools with different turnover rates, HSOC2 being more stabilized than
324 HSOC1 (Fig. 1b). The non-respired decomposed FOC is split between HSOC1 and HSOC2
325 following a parameter f_1. The non-respired decomposed HSOC1 is split between HSOC2 and
326 FOC following a parameter f_2 whereas non-respired decomposed HSOC2 is only redistributed
327 into the FOC pools. The decomposition of HSOC1 and HSOC2 both follow the equation (8)
328 but with different parameter values for a.
329
330 **2.5.2 Carbon transport mechanisms**
331 The transport of C between the different soil layers was represented by both advection and
332 diffusion mechanisms (Elzein and Balesdent, 1995), which have been shown to usually describe
333 well the C transport in soils (Bruun et al., 2007; Guenet et al., 2013). The advection represents
334 the C transport due to the water infiltration in the soil, while the diffusion represents the C

transport due to the fauna activity. The same transport coefficients were applied to the two C pools, FOC and HSOC.

The advection is defined by:

$$F_A = A \times C \qquad (9)$$

where F_A is the flux of *C* transported downwards by advection, and *A* is the advection rate (mm yr^{-1}).

The diffusion is represented by the Fick's law:

$$F_D = -D \times \frac{\partial^2 C}{\partial z^2} \qquad (10)$$

where F_D is the flux of C transported downwards by diffusion, $-D$ the diffusion coefficient (cm^2 yr^{-1}) and *C* the amount of carbon in the pool subject to transport (FOC or HSOC).

To represent the effect of soil tillage ($z \leq 0.2$ m), we added another diffusion term using the Fick's law but with a value of *D* several orders of magnitude higher to represent the mixing due to tillage. It must be noted that no tillage effect on the decomposition was represented here because of the large unknowns on these aspects (Dimassi et al., 2013; Virto et al., 2012).

In this model, the flux of *C* transported downwards by the advection and diffusion (F_{AD}) was represented as the sum of both mechanisms, following Elzein & Balesdent (1995):

$$F_{AD} = F_A + F_D \qquad (11)$$

The FOC and HSOC pools dynamics in the two pools model correspond to:

$$\frac{\partial FOC_{t,z,d}}{\partial t}$$

$$= I_{t,z,d} + \frac{\partial F_{AD}}{\partial z} + h \times \frac{\partial HSOC_{t,z,d}}{\partial t} dec\_HSOC_{t,z,d}$$

$$- dec\_FOC_{t,z,d} \frac{\partial FOC_{t,z,d}}{\partial t} \quad (12)$$

$$\frac{\partial HSOC_{t,z,d}}{\partial t}$$

$$= \frac{\partial F_{AD}}{\partial z} + h \times dec\_FOC_{t,z,d} \frac{\partial FOC_{t,z,d}}{\partial t}$$

$$- dec\_HSOC_{t,z,d} \frac{\partial HSOC_{t,z,d}}{\partial t} \quad (13)$$

Finally, the FOC, HSOC1 and HSOC2 pools dynamics in the three pools model correspond to:

$$\frac{\partial FOC_{t,z,d}}{\partial t}$$

$$= I_{t,z,d} + \frac{\partial F_{AD}}{\partial z} + h \times f_2 \times dec\_HSOC1_{t,z,d} \frac{\partial HSOC1_{t,z,d}}{\partial t} + h$$

$$\times dec\_HSOC2_{t,z,d} \frac{\partial HSOC2_{t,z,d}}{\partial t} - dec\_FOC_{t,z,d} \frac{\partial FOC_{t,z,d}}{\partial t} \quad (14)$$

$$\frac{\partial HSOC1}{\partial t \partial} = \frac{\partial F_{AD}}{\partial z} + h \times f_1 \times dec\_FOC_{t,z,d} \frac{\partial FOC_{t,z,d}}{\partial t}$$

$$- dec\_HSOC1_{t,z,d} \frac{\partial HSOC1_{t,z,d}}{\partial t} \quad (15)$$

$$\frac{\partial HSOC2}{\partial t} = \frac{\partial F_{AD}}{\partial z} + h \times (1 - f_1) \times dec\_FOC_{t,z,d} \frac{\partial FOC_{t,z,d}}{\partial t} + h \times (1 - f_2)$$

$$\times dec\_HSOC1_{t,z,d} \frac{\partial HSOC1_{t,z,d}}{\partial t} - dec\_HSOC2_{t,z,d} \frac{\partial HSOC2_{t,z,d}}{\partial t} \quad (16)$$

2.5.3 Depth dependence of HSOC potential decomposition rates

The shape of the function (i.e. the *b* parameter) describing the HSOC potential decomposition rate (Eq. (8)) was determined by incubating soils from the control, the alley and the tree row,

and from different soil layers (0.0-0.1, 0.1-0.3, 0.7-1.0 and 1.6-1.8 m). Soils were sieved at 5 mm, and incubated during 44 days at 20°C at a water potential of -0.03 MPa. Evolved CO_2 was measured using a micro-GC at 1, 3, 7, 14, 21, 28, 35, 44 days. The three first measurement dates corresponded to a pre-incubation period and were not included in the analysis. For a given depth, the cumulative mineralised SOC was expressed as a percentage of total SOC and was plotted against the incubation time. The slopes represented the potential SOC mineralisation rate at a given soil depth and location. The potential SOC mineralisation rates were then plotted against soil depth (Fig. S1). We used the soil incubations to determine only the *b* parameter of the curve: with such short term incubations, the SOC decomposition rate over the soil profile is overestimated because the CO_2 measured during the incubations mainly originates from the labile C pool. The *a* parameter was optimized following the procedure described further.

2.6 Boundary conditions of the CARBOSAF model

2.6.1 Annual aggregates of soil temperature and soil moisture

In April 2013, eight soil temperature and moisture sensors (Campbell CS 616 and Campbell 107, respectively) were installed in the agroforestry plot at 0.3, 1.3, 2.8 and 4.0 m depth, and at 2 and 5 m from the trees. Soil temperature and moisture were measured for 11 months.

The mean annual soil temperature in the agroforestry plot was described by the following equation:

$$T = -0.89 \times z + 288.24 \qquad (R^2 = 0.99) \qquad (17)$$

where T is the soil temperature (K) and z is the soil depth (m).

The mean annual soil moisture was described with the following equation:

$$\theta = 0.05 \times z + 0.28 \qquad (R^2 = 0.99) \qquad (18)$$

where θ is the soil volumetric moisture (cm cm^{-3}) and z is the soil depth (m).

Due to a lack of data in the agricultural plot, we assumed that the soil temperature and the soil moisture were the same in the agroforestry tree rows, alleys and in the control plot, but we further performed a sensitivity analysis of the model on these two parameters.

2.6.2 Interpolation of tree growth

The tree growth has been measured in the field since the establishment of the experiment. We used the diameter at breast height (*DBH*) as a surrogate of the tree growth preferentially to the tree height as the field measurements were more accurate. Indeed, *DBH* is easier to measure than height, especially when trees are getting older. To describe the temporal dynamic of *DBH* since the tree planting, a linear equation was fitted on the data.

Tree growth measurements enabled us to fit the following equation that was used in the model:

$$DBH_t \begin{cases} 0.01, & t \leq 3 \\ 0.0157 \times t - 0.0391 \ (R^2 = 0.997) & 3 < t \leq 20 \end{cases} \quad (19)$$

where DBH_t is the diameter at breast height (m) and t represents the time since tree planting (years).

2.6.3 Change of tree litterfall over time

For the five walnut trees where the leaf biomass was quantified, *DBH* was also measured. The ratio between the leaf biomass and *DBH* was then calculated for the five replicates. Total leaf biomass was 8.96 ± 1.45 kg DM tree^{-1} and the carbon concentration of walnut leaves was 449.4 ± 3.7 mg C g^{-1} (Table 2). With a density of 110 trees ha^{-1}, leaf litterfall was estimated at 0.73 ± 0.06 t C ha^{-1} in 2012 and at the plot scale. The ratio between leaf biomass and *DBH* was 0.0277 ± 0.0024 t C tree^{-1} m^{-1} or 3.05 t C ha^{-1} m^{-1}. The following linear relationship was therefore used in the model to describe leaf litter C input with the tree growth:

$$L_t = 3.05 \times DBH_t \quad (20)$$

where L_t is the leaf litter input (t C ha^{-1}) at the year *t*, and DBH_t the diameter at breast height (m) the year *t*.

2.6.4 Tree fine root C input from mortality

In 2012, the measured tree fine root biomass was higher in the tree row than in the alley (Table S1). From 0 to 1 m distance from the tree (in the tree row), the tree fine root biomass was homogeneous and was 1.01 t C ha^{-1} down 2 m depth.

In 2012 and in the alley, the tree fine root biomass (*TFRB*) decreased with increasing distance from the tree and was represented by an exponential function:

$$TFRB = \begin{cases} 1.01, & 0 \le d \le 1 \\ 1.29 \times e^{-0.28 \times d} \quad (R^2 = 0.90), & 1 < d \le 6.5 \end{cases} \qquad (21)$$

where *TFRB* represents tree fine root biomass down 2 m depth (t C ha^{-1}), and *d* the distance from the tree (m).

We considered a linear increase of *TFRB* with increasing *DBH*, and a linear regression was performed between *TFRB* in 2012 and *TFRB* in 1996, the first year after planting (biomass considered as negligible). The following linear relationship was used to simulate *TFRB* as a function of tree growth:

$$TFRB_{t,d} = \begin{cases} 3.69 \times DBH_t, & 0 \le d \le 1 \\ 4.70 \times DBH_t \times e^{-0.28 \times d}, & 1 < d \le 6.5 \end{cases} \qquad (22)$$

where $TFRB_t$ represents the tree fine root biomass to 2 m depth (t C ha^{-1}) at the year *t*, DBH_t the diameter at breast height (m) at the year *t*, and *d* the distance to the tree (m).

A changing distribution of tree fine roots within the soil profile was taken into account with increasing distance to the tree. For this purpose, exponential functions ($a \times e^{-b \times z}$) were fitted in the alley every 0.5 m distance, and a linear regression was fitted between their

coefficients *a* and *b* and distance from the tree. However, the distribution of *TFRB* within the soil profile and with the distance to the tree was considered constant with time.

A decreasing exponential function best represented the changing distribution of tree fine roots within the soil profile with increasing distance to the tree:

$$p_{TFRB,z,d} = \begin{cases} 13.92 \times e^{-1.39 \times z} \quad (R^2 = 0.68), & 0 \leq d \leq 1 \\ a \times e^{-b \times z}, & 1 < d \leq 6.5 \end{cases} \quad (23)$$

and

$$a = 10.31 - 1.15 \times d \quad (R^2 = 0.69) \quad (24)$$

$$b = -1.10 + 0.19 \times d \quad (R^2 = 0.51) \quad (25)$$

Finally,

$$p_{TFRB,z,d} = \begin{cases} 13.92 \times e^{-1.39 \times z}, & 0 \leq d \leq 1 \\ (10.31 - 1.15 \times d) \times e^{-(-1.10+0.19 \times d) \times z}, & 1 < d \leq 6.5 \end{cases} \quad (26)$$

where $p_{TFRB,z,d}$ is the proportion (%) of the total tree fine root biomass (*TFRB*) at a given depth *z* (m), and at a distance *d* from the tree (m).

To finally estimate the tree fine root input due to the mortality, *TFRB* was multiplied by the measured root turnover. The tree fine root turnover ranged from 1.7 to 2.8 yr^{-1} depending on fine root diameter, with an average turnover of 2.2 yr^{-1} for fine roots ≤ 2 mm and to a depth of 2 m (Germon et al., 2016).

2.6.5 Aboveground and belowground input from the crop

As there were more crop yield measurements (14) than straw biomass measurements (6), the effect of agroforestry on the crop yield with time was used as an estimate for change in the aboveground and belowground wheat biomass.

For this, the relative yield ($Rel\ Y_{AF}$) in the agroforestry system was calculated for each year as the ratio between the agroforestry yield and the control yield (Y_C).

The average annual crop yield in the control plot was $Y_C = 3.79 \pm 0.40$ t DM ha^{-1} for the 14 studied years. In the agroforestry plot, the average relative yield decreased linearly with time (increasing *DBH*) and was described using the following linear equation (Fig. 2):

$$Rel\ Y_{AF_t} = -93.33 \times DBH_t + 100 \qquad (R^2 = 0.12, \qquad p - value = 0.02) \qquad (27)$$

where $Rel\ Y_{AF_t}$ is the average relative crop yield (%) in the agroforestry plot compared to the control plot at year *t*, and DBH_t is the diameter at breast height (m) at year *t*.

The variation of crop yield with distance from the trees was described with a quadratic equation (Fig. 2). But as we aimed to predict SOC stocks up to 6.5 m distance from the trees (middle of the alley), a linear increase of crop yield with increasing distance from the tree gave similar results as the quadratic equation over the 6.5 m distance and was more parsimonious:

$$Rel\ Y_{AF_d} = 4.39 \times d + 64.57 \quad (R^2 = 0.24), \qquad 1 < d \leq 6.5 \qquad (28)$$

where $Rel\ Y_{AF_d}$ is the relative crop yield (%) in the agroforestry plot at a distance *d* (m) from the tree compared to the control plot.

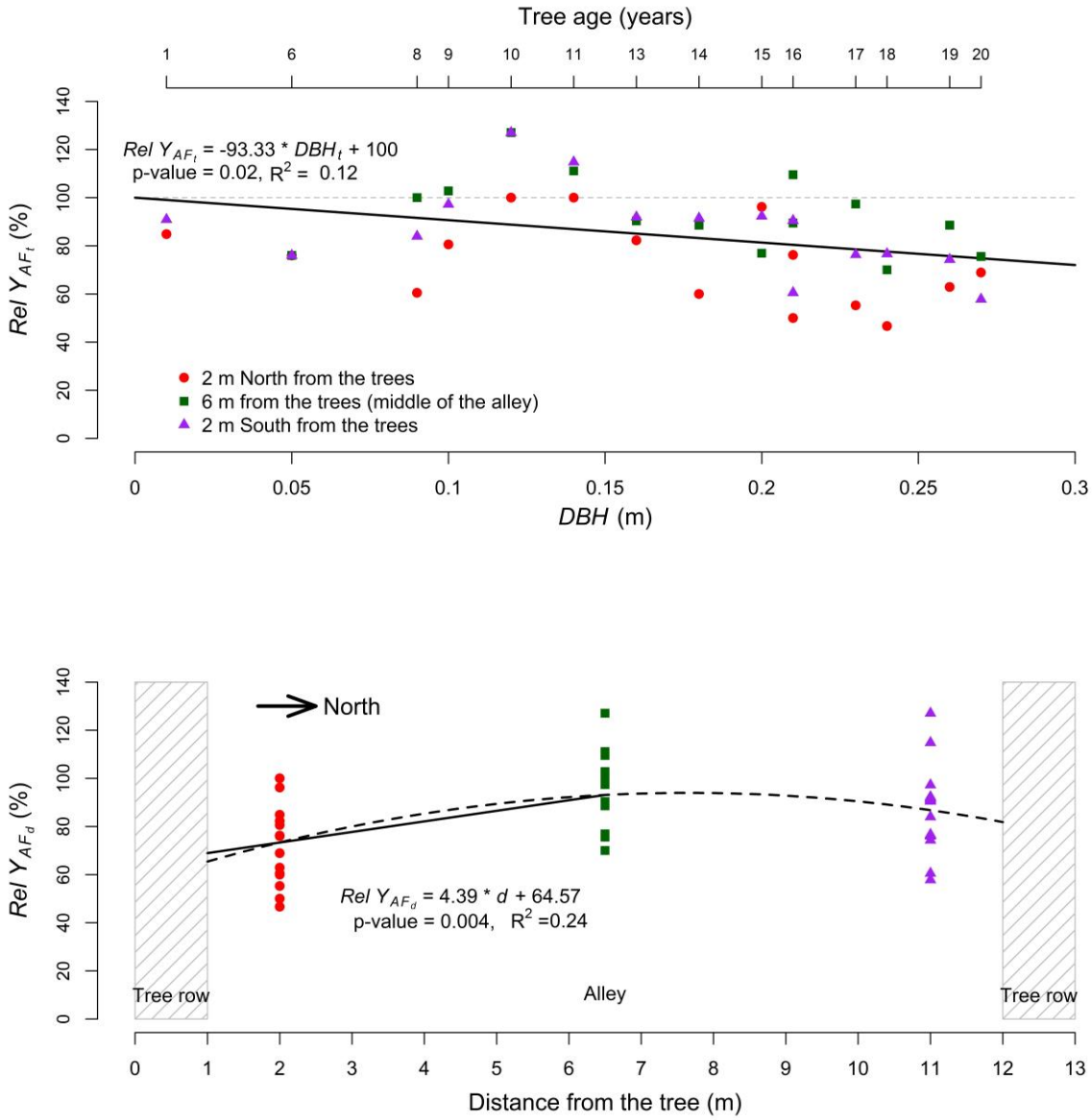

Fig. 2. Top: Relative yield ($Rel\ Y_{AF_t}$) in the agroforestry plot compared to the control plot as a function of tree growth, represented by the diameter at breast height (*DBH*) at year *t*. Bottom: Relative yield ($Y_{AF_{t,d}}$) as a function of the distance from the tree.

Finally, the crop yield in the agroforestry plot was modeled as follows:

$$Y_{AF_{t,d}} = Rel\ Y_{AF_t} \times Y_C \times Rel\ Y_{AF_d} \quad (R^2 = 0.19), \qquad 1 < d \leq 6.5 \qquad (29)$$

where $Y_{AF_{t,d}}$ is the crop yield (t DM ha^{-1}) in the agroforestry plot at the year *t* and at a distance *d* (m) from the tree. Because three linear equations were used to describe the crop yield in the

agroforestry plot, errors were accumulated and we finally came up with a standard underestimation of the crop yield in the agroforestry plot that we corrected by multiplying our equation by 1.2.

The ratio between the straw biomass and the crop yield was calculated as the average of the six measurements, and was considered constant with time. This ratio was used to convert crop yield into straw biomass. In the agroforestry plot, the carbon input to the soil from the aboveground crop biomass was:

$$ABC_{crop,t,d} = Y_{AF_{t,d}} \times (straw\ biomass{:}\ crop\ yield) \times C_{straw} \times (1 - export) \quad (30)$$

where $ABC_{crop,t,d}$ is the aboveground carbon input from the crop (t C ha^{-1}) at the year *t* and distance *d* from the tree, $Y_{AF_{t,d}}$ is the agroforestry crop yield. The average ratio between the straw biomass (t DM ha^{-1}) and the crop yield (t DM ha^{-1}) equaled 1.03 ± 0.11 (n=6). The wheat straw was exported out of the field after the harvest, but it was estimated that 25% of the straw biomass was left on the soil, thus *export*=0.75. In the control plot, $Y_{AF_{t,d}}$ was replaced by Y_C.

To estimate fine root biomass of the crop, we hypothesized that the root:shoot ratio of the durum wheat was the same in both the agroforestry and agricultural plot, in the absence of any published data on the matter. In the agroforestry plot, the belowground crop biomass was represented by:

$$BEC_{crop,t,d} = Y_{AF_{t,d}} \times (shoot{:}\ crop\ yield) \times (root{:}\ shoot) \times C_{root} \quad (31)$$

where $BEC_{crop,t,d}$ is the belowground crop biomass (t C ha^{-1}) at the year *t* and at a distance *d* from the tree, $Y_{AF_{t,d}}$ is the agroforestry crop yield. The average ratio between the total crop aboveground biomass (*shoot*) and the crop yield equaled 2.45 ± 0.15 (n=6). In 2012, total fine root biomass was 2.29 ± 0.32 t C ha^{-1} in the control (Table 3).

Table 3. Wheat fine root biomass in the agricultural control plot in 2012.

Soil depth (m)	Wheat fine root biomass (kg C m^{-3})	(t C ha^{-1})
0.0-0.1	0.48 ± 0.05	0.48 ± 0.05
0.1-0.3	0.34 ± 0.04	0.69 ± 0.09
0.3-0.5	0.22 ± 0.04	0.44 ± 0.08
0.5-1.0	0.10 ± 0.04	0.52 ± 0.20
1.0-1.5	0.03 ± 0.04	0.17 ± 0.19
Total	-	2.29 ± 0.32

522 Errors represent standard errors.

523

524 Therefore, the wheat *root:shoot* ratio equaled 0.79 ± 0.12 (n=1). The carbon concentration of
525 wheat root was C_{root} = 35.14 ± 1.90 mg C g^{-1}. In the control plot, $Y_{AF_{t,d}}$ was replaced by Y_C.

526

527 In 2012, no wheat roots were observed below 1.5 m, and root biomass decreased exponentially
528 with increasing depth (Table 3). The distribution of crop roots within the soil profile was
529 described as follows:

530 $$p_{CRBc,z} = \begin{cases} 26.44 \times e^{-2.59 \times z} \quad (R^2 = 0.99), & z \leq 1.5 \\ 0, & z > 1.5 \end{cases} \qquad (32)$$

531 where $p_{CRBc,z}$ is the proportion (%) of total crop root biomass in the control plot at a given
532 depth *z* (m).
533 Since the same maximum rooting depth of the crop was observed in the agroforestry plot and
534 in the control plot, we inferred that the wheat root distribution within the soil profile was not
535 modified by agroforestry, but only its biomass. The crop root turnover was assumed to be 1 yr^{-1}
536 , root mortality occurring mainly after crop harvest.

537

538

539 **2.6.6 Aboveground and belowground input from herbaceous vegetation in the tree rows**

540 The distance from the trees had no effect on the above and belowground biomass of the
541 herbaceous vegetation (data not shown), therefore average values are presented. The summer

aboveground biomass was almost three times higher than in winter, whereas the belowground biomass was two times higher (Table 4). The total aboveground carbon input was 2.13 ± 0.14 t C ha^{-1} yr^{-1} and the total belowground carbon input was 0.74 ± 0.05 t C ha^{-1} yr^{-1} to 0.5 m depth.

Table 4. Aboveground and belowground biomass of the herbaceous vegetation in the tree rows.

		Herbaceous biomass (t C ha^{-1})	
	Soil depth (m)	Summer	Winter
Aboveground	-	1.57 ± 0.11	0.56 ± 0.09
Belowground	0.0-0.1	0.22 ± 0.03	0.17 ± 0.01
	0.1-0.3	0.16 ± 0.02	0.06 ± 0.01
	0.3-0.5	0.09 ± 0.04	0.04 ± 0.01
	Total	0.46 ± 0.04	0.27 ± 0.02

Errors represent standard errors.

The belowground carbon input from the tree row vegetation ($BEC_{veg,z}$, t C ha^{-1}) at a given depth z (m) was described by the following equation:

$$BEC_{veg,z} = \begin{cases} 0.44 \times e^{-3.12 \times z}, & z \leq 1.5 \\ 0, & z > 1.5 \end{cases} \quad (33)$$

We assumed for simplification that the aboveground and belowground biomasses of the herbaceous vegetation in the tree row were constant over time.

2.7 Optimization procedure

Depending on the model variant, four to five parameters were optimized with a Bayesian statistical method (Santaren et al., 2007; Tarantola, 1987, 2005) using measured SOC stocks from the control plot only. These parameters were A, the advection rate, D, the diffusion coefficient, h the humification yield, a the coefficient of the k_{HSOC} rate from Eq. (10), and PE the priming coefficient. These four or five parameters were calibrated so that equilibrium SOC stocks, i.e. after 5000 years of simulation, equaled SOC stocks of the control plot in 2013. The associated uncertainty was estimated with the 93 soil cores sampled in the control plot (see

section 2.2.1). Due to a lack of relevant data, we assumed that the climate and the land use were the same for the last 5000 years, and that SOC stocks in the control plot were at equilibrium at the time of measurement. Therefore, SOC stocks at the end of the 5000 years of simulation equaled SOC stocks in the control plot. Three different calibrations were performed, corresponding to the three different models that were used: one calibration with the two pools model without the priming effect, one calibration with the two pools model with the priming effect, and one calibration with the three pools model.

Each model variant was fitted to the control SOC stocks data using a Bayesian curve fitting method described in Tarantola (1987), after a conversion from SOC stocks in kg C m^{-2} to SOC stocks in kg m^{-3} due to the different soil layers' thickness. We aimed to find a parameter set that minimizes the distance between model outputs and the corresponding observations, considering model and data uncertainties, and prior information on parameters. With the assumption of Gaussian errors for both the observations and the prior parameters, the optimal parameter set corresponds to the minimum of the cost function $\boldsymbol{J}(\boldsymbol{x})$:

$$\boldsymbol{J}(\boldsymbol{x}) = 0.5 \times \left[(\boldsymbol{y} - \boldsymbol{H}(\boldsymbol{x}))^t \times \boldsymbol{R}^{-1} \times \left(\boldsymbol{y} - \boldsymbol{H}(\boldsymbol{x})\right) + (\boldsymbol{x} - \boldsymbol{x}_b)^t \times {\boldsymbol{P}_b}^{-1} \times (\boldsymbol{x} - \boldsymbol{x}_b)\right] \quad (34)$$

that contains both the mismatch between modelled and observed SOC stock and the mismatch between a priori and optimized parameters. $\boldsymbol{x}$ is the vector of unknown parameters, $\boldsymbol{x}_b$ the vector of a priori parameter values, $\boldsymbol{H()}$ the model and y the vector of observations. The covariance matrices $\boldsymbol{P}_b$ and $\boldsymbol{R}$ describe a priori uncertainties on parameters, and observations, respectively. Both matrices are diagonal as we suppose the observation uncertainties and the parameter uncertainties to be independent. To determine an optimal set of parameters which minimizes $\boldsymbol{J}(\boldsymbol{x})$, we used the BFGS gradient-based algorithm (Tarantola, 1987). For each model variant, we performed 30 optimizations starting with different parameter prior values to check that the results did not correspond to a local minimum. As the BFGS algorithm does not directly

calculate the variance of posteriors, they were quantified using the curvature cost function at its minimum once it was reached (Santaren et al., 2007).

2.8 Comparison of models

Model predictions with and without priming effect were compared calculating the coefficients of determination, root mean square errors (RMSE) and Bayesian information criteria (BIC).

$$RMSE = \sqrt{\frac{1}{N}\sum_{i=1}^{N}(x_i - \bar{x})^2} \qquad (35)$$

where i is the number of observations (1 to N), x_i is the predicted value and $\bar{x}$ is the mean observed value.

$$BIC = \sim\sim N \times \ln(MSD) + k \sim\sim \times \ln(N) - 2 \times ln(\hat{L}) \qquad (36)$$

where N is the number of observations, ~~MSD is the mean squared deviation used to estimate the maximum likelihood (Manzoni et al., 2012), and~~ k is the number of model parameters, and $\hat{L}$ is the maximized value of the likelihood function of the model (Schwarz, 1978).

The model was run at a yearly time step using mean annual soil temperature and moisture and annual C inputs to the soil. In the agroforestry, the model was run from the ground (0 m) to 2 m depth, and from the tree (0 m) to 6.5 m from the tree (middle of the alley). The model was applied separately across locations of a tree-distance gradient having varying OC inputs, each soil column was considered independent from another. SOC pools were initialized after a spin-up of 5000 years in the control plot. At t_0, SOC stocks in the agroforestry plot therefore equaled SOC stocks of the control plot. The model was then run from t_0 to t_{18} (years) after tree planting. The spatial resolution was 0.1 m both vertically and horizontally. The model was developed

using R 3.1.1 (R Development Core Team, 2013). Partial-differential equations were solved using the R package *deSolve* and the *ode.1D* method (Soetaert et al., 2010).

2.9 Estimation of the priming intensity and its impact on SOC storage

In equation (7), the priming effect (*PE*) is considered as a control of the FOC on the HSOC decomposition and not as an accelerating factor of the HSOC decomposition. This method followed the Wutzler & Reichstein, (2008) approach based on the microbial biomass and adapted to the FOC by Guenet *et al.*, (2013) for models without explicit microbial biomass. Models able to reproduce priming effect generally need an explicit microbial biomass controlling the decomposition (Blagodatsky et al., 2010; Perveen et al., 2014). The priming scheme used here allows some simplifications in the model structure since an explicit representation of the microbial biomass is not needed. Furthermore, at equilibrium state (i.e. when the input rate is constant) the decomposition rate of a first order equation (Eq. (6)) takes *PE* implicitly into account. Indeed, when FOC enters the system, there is an induced priming, a constant FOC input rate therefore induces a constant priming. This means that when we optimized the decomposition rate parameter in the control plot, we implicitly represented this priming but at a fixed rate. When FOC inputs are modified, due to the tree growth for instance, the *PE* intensity is modified and this effect cannot be represented by classical first order kinetics. To estimate the importance of priming on SOC storage in the agroforestry plot, the simulations using first order equations (Eq. (6)) can therefore not be directly compared to the simulations using the FOC-dependant decomposition rate (Eq. (7)). To estimate the change of SOC decomposition rate due to priming when trees are planted, the decomposition fluxes predicted by Eq. (7) $\left(-k_{HSOC,z} \times (1 - e^{-PE \times FOC_{t,z,a}})\right)$ in the agroforestry plot must be compared to the fluxes in the agroforestry plot using the decomposition rate from the control plot calculated by Eq. (7) with $FOC_{t,z,a}$ corresponding to the FOC inputs in the control plot.

~~Thus, to calculate the importance of priming on SOC storage when trees are planted, we used the decomposition rates calculated following Eq. (7) in the control plot $\left(-k_{HSOC,z} \times (1 - e^{-PE \times FOC_{tzd}})\right)$ and we applied this decomposition rate to the agroforestry plot as a classical first order kinetics (without the control FOC, i.e. $k_{new} = -k_{HSOC,z} \times (1 - e^{-PE \times FOC_{tzd}})$ with $FOC_{t,z,d}$ fixed constant). This simulation corresponded to the absence of priming due to trees in the agroforestry plot (i.e. decomposition not controlled by the FOC of the agroforestry plot). By difference with the simulation performed with the full two pools model (Eq. (7)), i.e., taking account of FOC input and priming, we calculated the priming intensity.~~

3 Results

3.1 Organic carbon inputs and SOC stocks: a synthesis from field measurements

In the alleys of the18-year-old agroforestry system, measured organic carbon (OC) inputs from the crop residues and roots were reduced compared to the control plot due a lower crop yield (Fig. 3). This reduction in crop OC inputs was offset by OC inputs from the tree roots and tree litterfall. Total root OC inputs in the alleys (crop + tree roots) and in the control plot (crop roots) were very similar, respectively 2.43 and 2.29 t C ha^{-1} yr^{-1}. Alleys received 0.60 t C ha^{-1} yr^{-1} more of total aboveground biomass (crop residues + tree litterfall) than the control, which was added to the plough layer. Tree rows received 2.35 t C ha^{-1} yr^{-1} more C inputs in the first 0.3 m of soil compared to the control plot, mainly from the herbaceous vegetation. Down the whole soil profile, ~~T~~tree rows ~~in the agroforestry system~~ received two times more ~~organic carbon (~~OC~~)~~ inputs compared to the control plot (Fig. 3), and 65% more than alleys. Overall, the agroforestry plot had 41% more OC inputs to the soil than the control plot to 2 m depth (3.80 t C ha^{-1} yr^{-1} compared to 2.69 t C ha^{-1} yr^{-1}). In the agroforestry plot, the largest aboveground OC input to the soil comes from the herbaceous vegetation, and not from the trees. In the control plot, 85%

of OC inputs are wheat root litters. In the agroforestry plot, root inputs represent 71% of OC inputs in the alleys, and 50% in the tree rows.

In the first 0.3 m of soil, SOC stocks were significantly higher in the alleys than in the control plot, but the difference was small (2.1 ± 0.6 t C ha^{-1}). Between 0.3 and 1.0 m, the difference of SOC stocks was smaller but still significant. However, between 1 and 2 m depth, SOC stocks were significantly lower in the alleys than in the control. As a consequence, there was no significant difference of total SOC stocks between the two locations down the whole soil profile. In the tree rows, topsoil organic carbon stocks (0.0-0.3 m) were much higher than in the control (+ 17.0 ± 1.4 t C ha^{-1}). This positive difference of SOC stocks decreased with depth but remained significantly positive down 1.5 m depth. The opposite was observed between 1.5 and 2.0 m depth. Delta of total SOC stocks between the tree rows and the control plot was 20.1 ± 1.6 t C ha^{-1}. At the plot scale, total SOC stocks were significantly higher in the agroforestry plot compared to the control plot down 2 m depth (+ 3.3 ± 0.9 t C ha^{-1}).

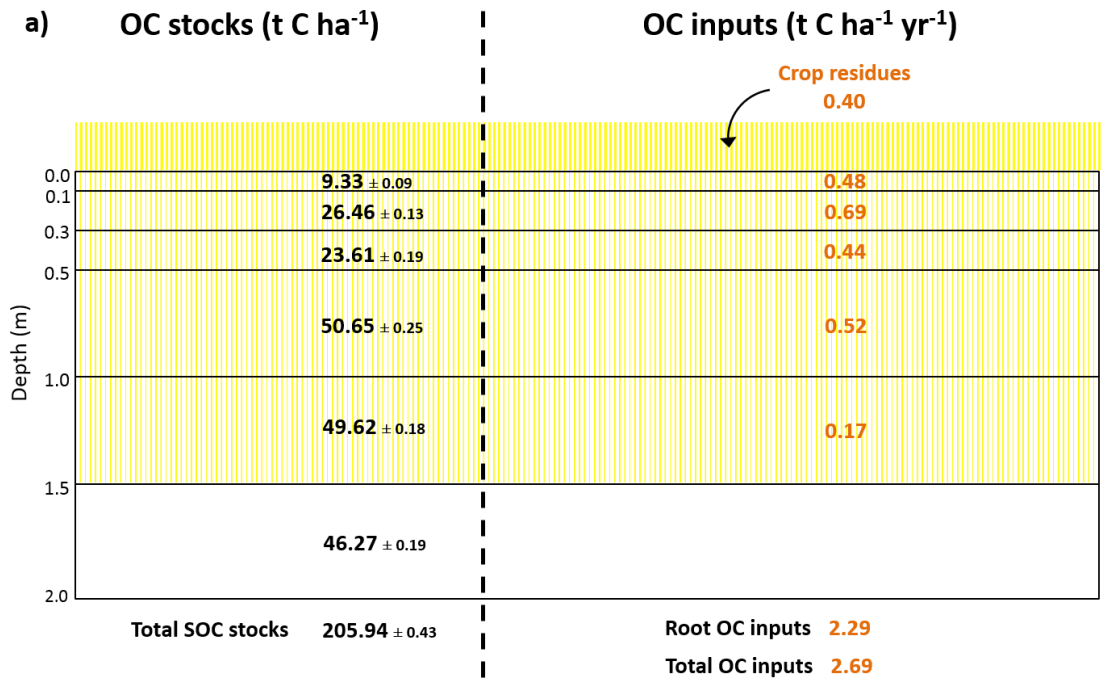

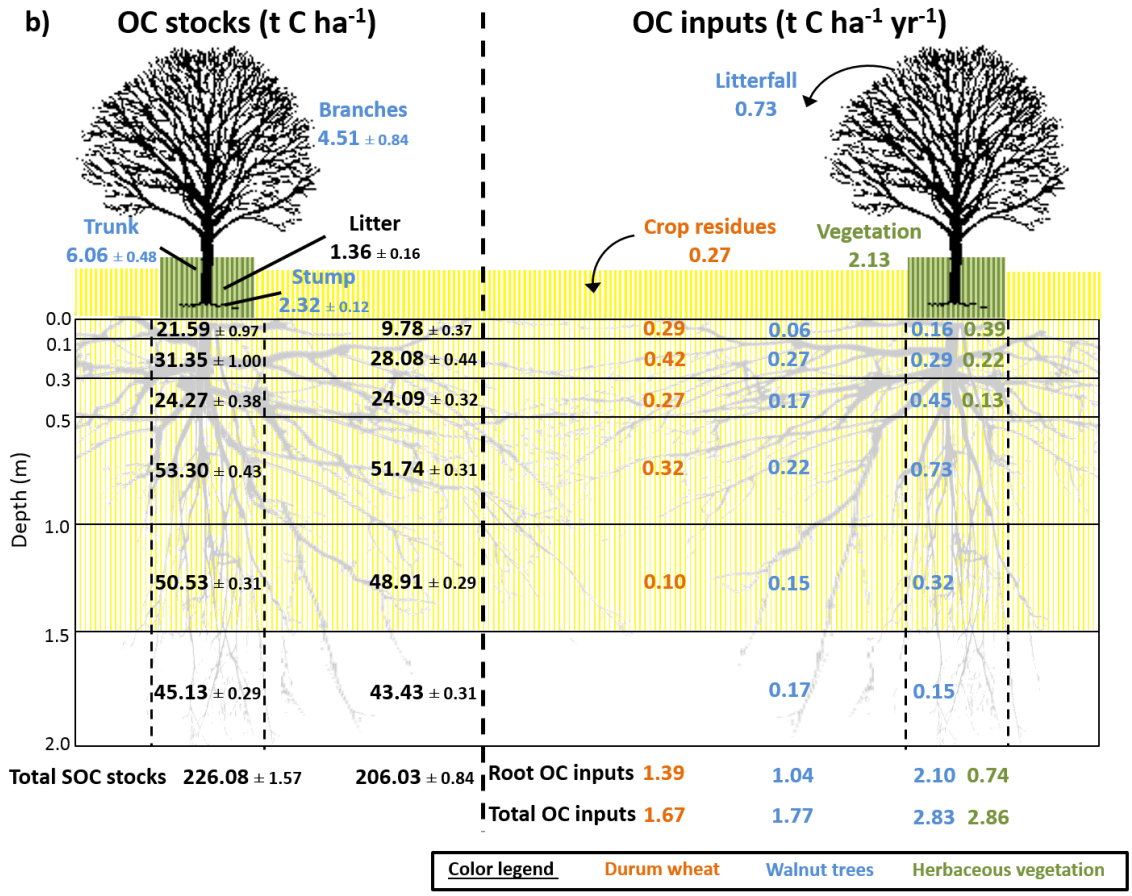

Fig. 3. Measured soil organic carbon stocks and organic carbon inputs to the soil a) in the agricultural control plot, b) in the 18-year-old agroforestry plot. Associated errors are standard errors. Values are expressed per hectare of land type (control, alley, tree row). To get the values per hectare of agroforestry, data from alley and tree row have to be weighted by their respective surface area (i.e., 84% and 16%, respectively) and then added up. OC: organic carbon; SOC: soil organic carbon. SOC stocks data are issued from Cardinael *et al.*, (2015a), data of tree root OC inputs are combined from Cardinael *et al.*, (2015b) and from Germon *et al.*, (2016).

3.2 HSOC decomposition rate

The soil incubation experiment showed that the HSOC mineralization rate decreased exponentially with depth (Fig. S1) and could be described with:

$$k_{HSOC,z} = 6.114 \times e^{-1.37 \times z} \quad (R^2 = 0.76) \qquad (374)$$

where z is the soil depth (m), and where the a (yr^{-1}) coefficient (a = 6.114) was further optimized (Table 5).

Table 5. Summary of optimized model parameters.

Model parameter	Meaning	Prior range (log)*	Posterior values ± variance (prior values)		
			2 pools - without *PE*	2 pools - with *PE*	3 pools – without *PE*
a	coefficient from Eq. (8) of the HSOC decomposition (yr^{-1})	~~$3.65e^{-6}$~~ - 12.52 - ~~3.65~~1.29	$0.01e^{-2} \pm <10^{-4}$ ($0.01e^{-2}$)	$0.01e^{-2} \pm <10^{-4}$ ($0.01e^{-2}$)	-
a_1	coefficient from Eq. (8) of the HSOC1 decomposition (yr^{-1})	~~$3.65e^{-6}$~~ - 12.52 - ~~3.65~~1.29	-	-	$0.01e^{-2} \pm <10^{-4}$ ($0.01e^{-2}$)
a_2	coefficient from Eq. (8) of the HSOC2 decomposition (yr^{-1})	~~$3.65e^{-6}$~~ - 12.52 - ~~3.65~~1.29	-	-	$0.83e^{-2} \pm 0.17e^{-2}$ ($0.83e^{-2}$)
D	diffusion coefficient ($cm^2\ yr^{-1}$)	~~$1e^{-6}$~~ - 13.82 - ~~1~~0	$4.62e^{-4} \pm 5.95e^{-4}$ ($9.64e^{-4}$)	$5.63e^{-4} \pm 1.42e^{-4}$ ($9.01e^{-4}$)	$5.24e^{-4} \pm 7.62e^{-4}$ ($9.64e^{-4}$)
A	advection rate ($mm\ yr^{-1}$)	~~$1e^{-6}$~~ - 13.82 - ~~1~~0	$21.25e^{-4} \pm 5.02e^{-4}$ ($8.54e^{-4}$)	$6.63e^{-4} \pm 2.38e^{-4}$ ($4.27e^{-4}$)	$21.60e^{-4} \pm 2.24e^{-4}$ ($8.54e^{-4}$)
h	humification yield	~~0.01~~ - 4.61 - ~~1~~0	$0.32 \pm <10^{-4}$ (0.34)	$0.25 \pm 1.00e^{-4}$ (0.13)	0.34 ± 0.03 (0.34)
PE	priming coefficient	~~0.1~~ - 2.30 - ~~160~~5.08	-	9.66 ± 1.49 (102.95)	-
f_1	fraction of decomposed FOC entering the HSOC1 pool	0-1	-	-	0.99 ± 0.18 (0.86)
f_2	fraction of decomposed HSOC1 entering the FOC pool	0-1	-	-	$0.94 \pm 1.10e^{-3}$ (0.80)

The prior range represents the range in which prior values were sampled for the 30 optimizations per model variant. The prior values presented in brackets in the posterior column represent the prior values that minimized the **J(x)** value (Eq. (34)). * Except for f_1 and f_2.

694

3.3 Modeling results

3.3.1 Optimized parameters and correlation matrix

The optimized parameters and their prior modes are presented in Table 5. For the two pools model without priming effect, the most important correlation was observed between *h* and *A* which control the humification and the transport by advection. Concerning the two pools model with priming effect, the most important correlations were observed between *h* and *PE* which controls the effect of the FOC on HSOC decomposition, and between *h* and *A*. *A* and *PE* were also positively correlated (Fig. S2). For the three pools model, f_1 and f_2 were by definition negatively correlated, but f_2 and *A* were also correlated. Considering the method used to optimize the parameters, these important correlation factors hinder the presentation of the model output within an envelope. Therefore, we presented the model results using the optimized parameter without any envelope.

3.3.2 Modeled SOC stocks

As a reminder, SOC stocks of the agroforestry plot were not part of model calibration (that used the control plot only) but were used here for validation. Observed SOC stocks were not well represented by the two pools model without priming effect, with RMSE ranging from 1.00 to 1.07 kg C m^{-3} (Fig. 4, Table S2). The model performed better when the priming effect was taken into account, with RMSE ranging from 0.41 to 0.95 kg C m^{-3}, and the SOC profile was well described. The representation of SOC stocks was not improved by the inclusion of a third C pool in the model. Overall, the two pools model with priming effect was the best one, as shown by the BICs (Fig. 4, Table S2). For all models, SOC stocks below 1 m depth were better described than above SOC stocks (Table S2). The spatial distribution of SOC stocks and of additional SOC storage was also well described (Fig. 5), with a very high additional SOC storage in the topsoil layer in the tree row. Most modeled SOC storage in the agroforestry plot

720 was located in the first 0.2 m depth, but SOC storage was slightly higher in the middle of the
721 alleys than in the alleys close to the tree rows.

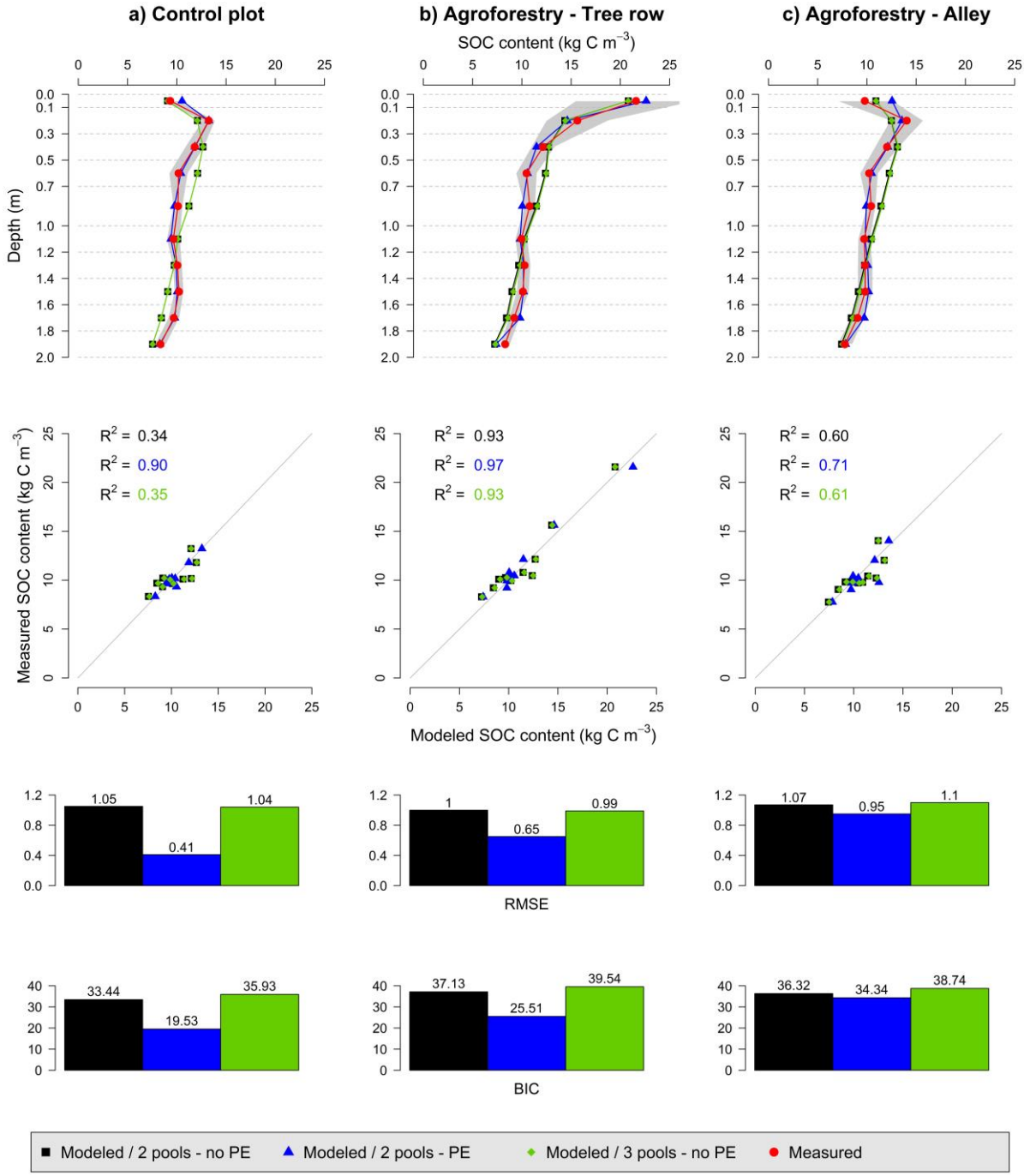

722

723 **Fig. 4.** Measured and modeled soil organic carbon contents (kg C m^{-3}) in an agricultural control
724 plot and in an 18-year-old silvoarable system with a two pools model without priming effect
725 (no *PE*), with a two pools model with priming effect (*PE*) and with a three pools model without

PE. Gray shaded bands represent standard deviations of measured SOC stocks (n=93 in the control, n=40 in the tree rows, and n=60 in the alleys).

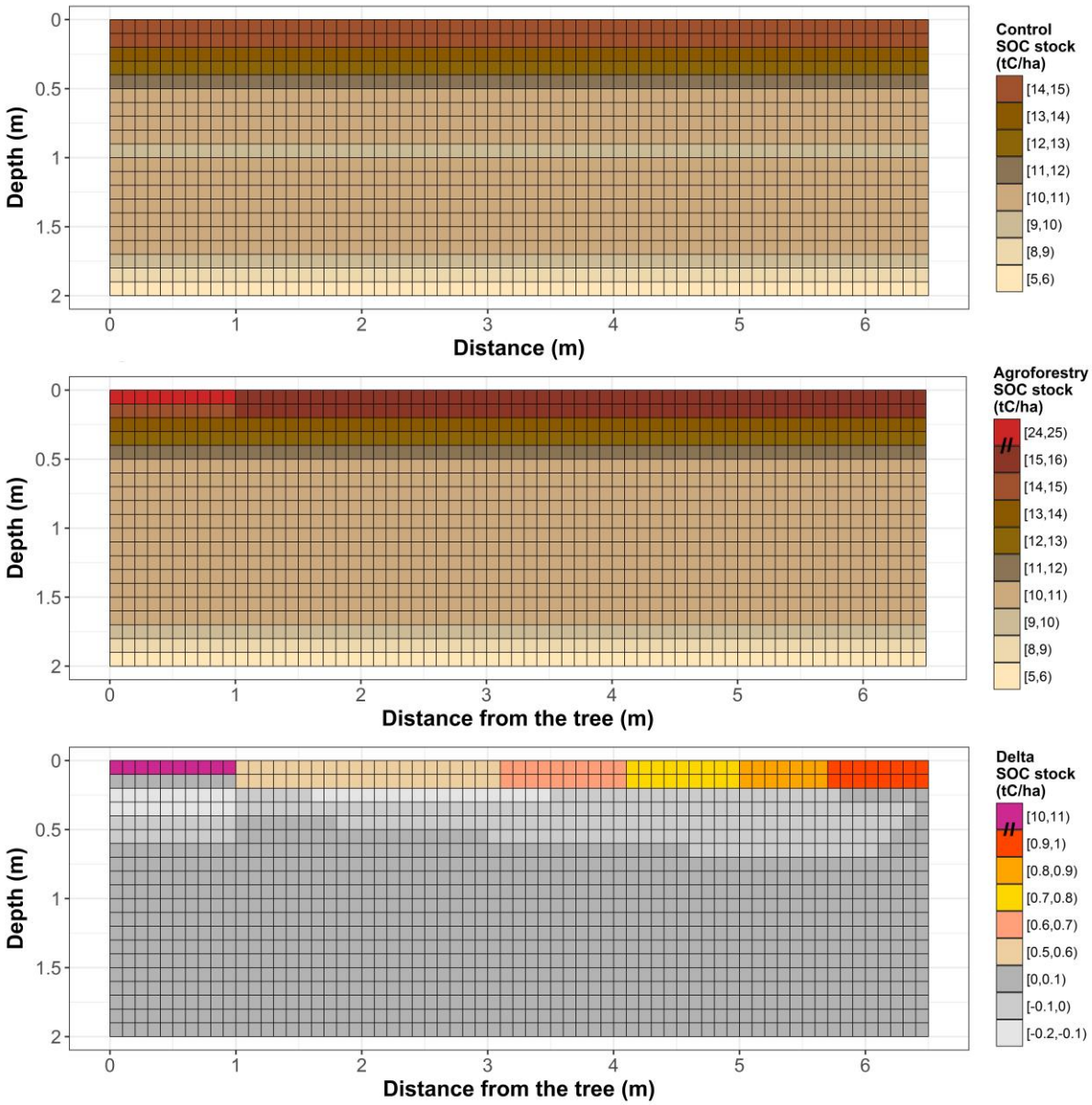

Fig. 5. Spatial distribution of control SOC stocks (top), agroforestry SOC stocks (middle), and additional SOC storage (t C ha^{-1}) in an 18-year-old silvoarable system compared to an agricultural control plot and represented by the two pools model with priming effect. The scale used in the middle and bottom panels are not continuous due to the large stocks predicted by the model in the top layer in the tree-row.

3.3.3 Antagonist effect of priming on SOC storage

The priming effect increases the decomposition rate when more FOC is available (Fontaine et al., 2007). Therefore, the effect of a C inputs increase on SOC storage in the agroforestry plot might be counterbalanced by priming. With our model we were able to estimate the contribution of each driver on SOC storage. The introduction of priming effect in the model reduced the potential SOC storage due to higher organic inputs in the agroforestry system by 91% in the alley, and by 76% in the tree rows (Fig. 6). The potential effect of OC inputs alone on SOC storage was 49.12 to 62.77 t C ha^{-1}, but the effect of priming on SOC storage was -44.89 to -47.67 t C ha^{-1}, resulting in a modeled SOC storage of 4.23 t C ha^{-1} in the alley and of 15.09 t C ha^{-1} in the tree row down 2 depth (Fig. 6). The negative effect of priming effect on SOC storage increased with increasing soil depth (Fig. S3).

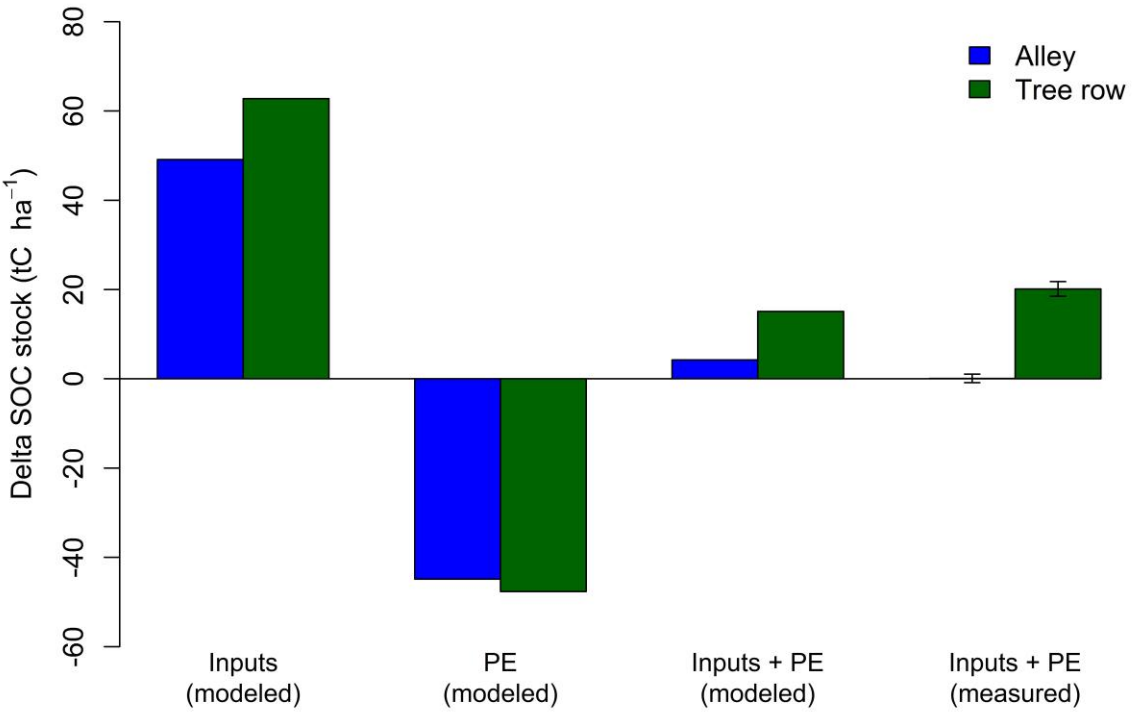

Fig. 6. Decoupling the role of C inputs and priming effect (*PE*) on SOC storage in an 18-year-old silvoarable system down 2 m depth. Inputs: only the input effect is modeled; *PE*:

~~only the priming effect is modeled; Inputs + *PE*: model prediction with both processes taken into account.~~

4 Discussion

4.1 OC inputs drive SOC storage in agroforestry systems

Increased SOC stocks in the agroforestry plot compared to the control may be explained either by increased OC inputs, or decreased OC outputs by SOC mineralization, or both. In the alleys, higher SOC stocks in the topsoil could be explained by inputs from litterfall and tree roots despite a decrease in crop inputs. Most of additional SOC storage in the agroforestry plot was found in the topsoil in the tree rows. The same distribution was observed for OC inputs to the soil. Inputs from the herbaceous vegetation had an important impact on SOC storage ~~in this agroforestry system~~. The increased SOC stocks in the tree rows were largely explained ~~in a big part~~ by an important above-ground carbon input (2.13 t C ha^{-1} yr^{-1}) by the herbaceous vegetation between trees. This result had already been suggested by Cardinael et al., (2015b) and by Cardinael et al., (2017) who showed that even young agroforestry systems could store SOC in the tree rows while trees are still very small. These "grass strips" indirectly introduced by the tree planting in parallel tree rows have a major impact on SOC stocks of agroforestry systems. Increased SOC stocks below the plough layer could be explained by higher root inputs, but these inputs could also have contributed to decrease SOC stocks below 1.5 m due to priming effect. At the plot scale, ~~M~~measured organic carbon inputs to the soil were increased by 40% (+1.1 t C ha^{-1} yr^{-1}) down ~~to~~ 2 m depth in the 18-year-old agroforestry plot compared to the control plot, resulting in increased SOC stocks of 3.3 t C ha^{-1}. Increased OC inputs in agroforestry systems has been shown in other studies but they were only quantified in the first 20 cm of soil (Oelbermann et al., 2006; Peichl et al., 2006). This study is therefore the first one also quantifying deep OC inputs to soil. In this study and due to a lack of data, soil temperature

and soil moisture were considered the same in both plots so that abiotic factors controlling SOC decomposition were identical. Reduced soil temperature is often observed in agroforestry systems (Clinch et al., 2009; Dubbert et al., 2014), but effect of agroforestry on soil moisture is much more complex. The soil evaporation is reduced under the trees, but soil water is also lost through the transpiration of trees (Ilstedt et al., 2016; Ong and Leakey, 1999). These opposing effects vary with the distance from the tree (Odhiambo et al., 2001). Moreover, increased water infiltration and water storage has been observed under the trees after a rainy event (Anderson et al., 2009). Therefore, the effect of agroforestry on soil moisture is variable in time and space, and should be investigated more in details. Interactions between soil temperature and soil moisture on the SOC decomposition are known to be complex (Conant et al., 2011; Moyano et al., 2013; Sierra et al., 2015). A sensitivity analysis performed on these two boundary conditions showed that the model was not very sensitive to soil temperature and soil moisture (Fig. S3), but the real effect of these two parameters on SOC dynamics under agroforestry systems should be specifically investigated in future studies. Despite these simplifying assumptions on similarities in microclimate but also on vertical transport between the control and the agroforestry system, the model calibrated to the control plot was able to reproduce SOC stocks in tree rows and alleys and its depth distribution well. This strong validation also ~~also suggests that~~revealed that OC inputs were sufficient to explain the differences in SOC stocks ~~is the main driver of SOC storage~~ at this site~~, and that a potential effect of agroforestry microclimate on SOC mineralization is of minor importance~~.. ~~Reduced soil temperature is often observed in agroforestry systems (Clinch et al., 2009; Dubbert et al., 2014), but effect of agroforestry on soil moisture is much more complex. The soil evaporation is reduced under the trees, but water is lost through their transpiration (Ilstedt et al., 2016; Ong and Leakey, 1999), and these effects vary with the distance from the tree (Odhiambo et al., 2001). Moreover, the water infiltration and the water storage can be increased under the trees after a rainy event (Anderson et al.,~~

~~2009). Therefore, the effect of agroforestry on soil moisture is variable in time and space, and should be investigated more in details. Interactions between soil temperature and soil moisture on the SOC decomposition are known to be complex (Conant et al., 2011; Moyano et al., 2013; Sierra et al., 2015) and up to now it is not possible to predict the effect of agroforestry microclimate on the SOC decomposition rate. A sensitivity analysis performed on these two boundary conditions showed that the model was not very sensitive to soil temperature and soil moisture (Fig. S4), but the real effect of these two parameters on SOC dynamics under agroforestry systems should be better investigated in future studies.~~ Furthermore, the SOC decomposition rate could also be modified due to an absence of soil tillage in the tree rows (Balesdent et al., 1990) or to an increased aggregate stability (Udawatta et al., 2008) in the topsoil.

4.2 Representation of SOC spatial heterogeneity in agroforestry systems

The lateral spatial heterogeneity of SOC stocks in the agroforestry plot was well described by the two pools model including priming effect, with higher SOC stocks in the tree rows' topsoil than in the alleys. ~~Inputs from the herbaceous vegetation had an important impact on SOC storage in this agroforestry system. The increased SOC stocks in the tree rows were explained in a big part by an important above-ground carbon input (2.13 t C ha^{-1} yr^{-1}) by the herbaceous vegetation between trees. This result had already been suggested by Cardinael et al., (2015b) and by Cardinael et al., (2017) who showed that even young agroforestry systems could store SOC in the tree rows while trees are still very small. These "grass strips" indirectly introduced by the tree planting in parallel tree rows have a major impact on SOC stocks of agroforestry systems.~~ The model treated the carbon from ~~this~~ the tree row herbaceous litter as an input to the upper layer of the mineral soil, in the same way as inputs by roots. Introduction of nitrogen in the model could be further tested in order to take into account a lower carbon use efficiency

due to a lack of nutrients for microbial growth in this litter. For all models, SOC stocks were better described in the tree rows than in the alleys. In the alleys, the spatial distribution of organic inputs is more complex and thus more difficult to model. The tree root system is influenced by the soil tillage and by the competition with the crop roots, and thus the highest tree fine root density is not observed in the topsoil but in the 0.3-0.5 m soil layer (Cardinael et al., 2015a). In the model, we were not able to represent this specific tree root pattern with commonly used mathematical functions, and tree root profiles were modeled, by default, using a decreasing exponential. Indeed, piecewise linear functions introduce threshold effects not desirable for transport mechanisms, especially diffusion. This simplification could partly explain the model overestimation of SOC stocks in the 0.0-0.1 m layer of the alleys compared to observed data. This result suggests that it could be useful to couple the CARBOSAF model with a model describing root architecture and root growth (Dunbabin et al., 2013; Dupuy et al., 2010), using for instance voxel automata (Mulia et al., 2010). Moreover, the model described a slight increase of SOC stocks in the middle of the alleys than close to the trees in the alleys. This could be explained by the linear equation used to describe the crop yield as a function of the distance from the trees, leading to an overestimation of the crop yield reduction close to the trees. It could also be explained by the formalism used to model leaf litter distribution in the plot. We considered a homogeneous distribution of leaf inputs in the agroforestry plot, which was the case in the last years, but probably not in the first years of the tree growth where leaves might be more concentrated close to the trees (Thevathasan and Gordon, 1997).

The two pools model with priming effect also represented a slight SOC storage in the agroforestry plot below 1.0 m depth, but it was not observed in the field. This could be linked to an overestimation of C input from tree fine root mortality. Indeed, a constant root turnover was considered along the soil profile, but several authors reported a decrease of the root turnover with increasing soil depth (Germon et al., 2016; Hendrick and Pregitzer, 1996; Joslin

et al., 2006). However, the sensitivity analysis showed that the model was not sensitive to this parameter (Fig. S34).

4.3 Vertical representation of SOC profiles in models

The best model to represent SOC profiles considered the priming effect. This process can act in two different ways on the shape of SOC profiles. It has a direct effect on the SOC mineralization and it therefore modulates the amount of SOC in each soil layer, creating different SOC gradients. This indirectly affects the mechanisms of C transport within the soil profile, as shown by a modification of transport coefficients in the case of priming effect (Table 5). Contrary to what was shown by Cardinael *et al.*, (2015c) in long term bare fallows receiving contrasted organic amendments, the addition of another SOC pool could not surpass the inclusion of priming effect in terms of model performance. Together with Wutzler & Reichstein, (2013) and Guenet *et al.*, (2016), this study therefore suggests that implementing priming effect into SOC models would improve model performances especially when modelling deep SOC profiles.

We considered here the same transport coefficients for the FOC and HSOC pools, but the quality and the size of OC particles are different, potentially leading to various movements in the soil by water fluxes or fauna activity (Lavelle, 1997). Moreover, we considered identical transport parameters in the agroforestry and in the control plot, but the presence of trees could modify soil structure, soil water fluxes (Anderson et al., 2009), and the fauna activity (Price and Gordon, 1999). However, the model was little sensitive to these parameters (Fig. S34). Further study could investigate the role of different transport coefficients on the description of SOC profiles.

4.4 Higher OC inputs or a different quality of OC?

The introduction of trees in an agricultural field not only modifies the amount of litter residues, but also their quality. Tree leaves, tree roots, and the herbaceous vegetation from the tree row have different C:N ratios, lignin and cellulose contents than the crop residues. Recent studies showed that plant diversity had a positive impact on SOC storage (Lange et al., 2015; Steinbeiss et al., 2008). One of the hypothesis proposed by the authors is that diverse plant communities result in more active, more abundant and more diverse microbial communities, increasing microbial products that can potentially be stabilized. In our model, litter quality is not related to different SOC pools, but is implicitly taken into account in the FOC decomposition rate, which is weighted by the respective contribution from the different types of OC inputs. To test this, we performed a model run considering that all OC inputs in the agroforestry plot were crop inputs (all FOC decomposition rates equaled wheat decomposition rate), but results were not significantly different from the one presented here. ~~We then~~Hence, we consider~~ed~~ that changes in litter quality in the agroforestry plot did not significantly influence SOC decomposition rates.

4.5 Possible limitation of SOC storage by priming effect

Our modelling results ~~showed~~ suggested that the priming effect could considerably reduce the capacity of soils to store organic carbon. Our study showed that the increase of SOC stocks was not proportional to OC inputs, especially at depth. This result has often been observed in Free Air CO_2 Enrichment (FACE) experiments. In these experiments, productivity is usually increased due to CO_2 fertilization, but several authors also reported an increase in SOC decomposition but not linearly linked to the productivity increase (van Groenigen et al., 2014; Sulman et al., 2014). ~~In this study, the estimation of the priming effect intensity was possible because most OC inputs to the soil were accurately measured. The modelled intensity of priming effect was very strong, offsetting 75 to 90% of potential SOC storage due to OC inputs.~~ In a long-term FACE experiment, Carney *et al.*, (2007) also found that SOC decreased due to

898 priming effect, offsetting 52% of additional carbon accumulated in aboveground and coarse
899 root biomass. The priming effect intensity also relies on nutrient availability (Zhang et al.,
900 2013). In agroforestry systems, tree roots can intercept leached nitrate below the crop rooting
901 zone (Andrianarisoa et al., 2016), reducing nutrient availability. This beneficial ecosystem
902 service could indirectly increase the priming effect intensity in deep soil layers.
903 ~~However, this strong intensity could also partially be linked to the formalism used to simulate~~
904 ~~priming effect. This~~ The formalism used here to simulate priming effect assumes that there is
905 no mineralisation of the SOC in the absence of fresh OC inputs (no basal respiration). This is a
906 strong hypothesis, but this situation never occurs since the FOC pool is never empty (data not
907 shown). In the alleys and below the maximum rooting depth of crops, there are no direct inputs
908 of FOC, but OC is transported in these deep layers due to transport mechanisms. However,
909 further studies could study the impact of the priming effect formalism on the estimation of its
910 intensity by using explicit microbial biomass for instance (Blagodatsky et al., 2010; Perveen et
911 al., 2014).
912 Finally, root exudates were not quantified in this study. Several authors showed that they could
913 induce strong priming effects (Bengtson et al., 2012; Keiluweit et al., 2015), but root exudates
914 are also a source of labile carbon, potentially contributing to stable SOC (Cotrufo et al., 2013).
915 These opposing effects of root exudates on SOC should be further investigated, especially
916 concerning the deep roots in agroforestry systems.
917
918 **5 Conclusions**
919 We proposed the first model that simulates soil organic carbon dynamics in agroforestry
920 accounting for both the whole soil profile and the lateral spatial heterogeneity in agroforestry
921 plots. The two pools model with priming effect described reasonably well the measured SOC
922 stocks after 18 years of agroforestry and SOC distributions with depth. It showed that the

increased inputs of fresh biomass to soil in the agroforestry system explained the observed additional SOC storage and suggested priming effect as a process controlling SOC stocks in the presence of trees. This study points out at processes that may be modified by deep rooting trees and deserve further studies given their potential effects on SOC dynamics, such as additional inputs of C as roots exudates, or altered soil structure leading to modified SOC transport rates.

6 Data availability

The data and the model are freely available upon request and can be obtained by contacting the author (remi.cardinael@cirad.fr).

Information about the Supplement

The Supplement includes the walnut tree fine root biomass (Table S1), the different model performances (Table S2), the potential SOC decomposition rate as a function of soil depth (Fig. S1), the correlation matrix of optimized parameters (Fig. S2), ~~the decoupling of OC inputs and priming effect as a function of soil depth (Fig. S3),~~ and a sensitivity analysis of the model (Fig. S3~~4~~).

Acknowledgments.

This study was financed by the French Environment and Energy Management Agency (ADEME), following a call for proposals as part of the REACCTIF program (Research on Climate Change Mitigation in Agriculture and Forestry). This work was part of the funded project AGRIPSOL (Agroforestry for Soil Protection, 1260C0042), coordinated by Agroof. Rémi Cardinael was supported both by ADEME and by La Fondation de France. We thank the farmer, Mr Breton, who allowed us to sample in his field. We are very grateful to our colleagues for their work in the field since the tree planting, especially Jean-François Bourdoncle, Myriam

Dauzat, Lydie Dufour, Jonathan Mineau, Alain Sellier and Benoit Suard. We thank colleagues and students who helped us for measurements in the field or in the laboratory, especially Daniel Billiou, Cyril Girardin, Patricia Mahafaka, Agnès Martin, Valérie Pouteau, Alexandre Rosa, and Manon Villeneuve. Finally, we would like to thank Jérôme Balesdent, ~~and~~ Pierre Barré and Philippe Peylin for their valuable comments on the modeling part of this work.

References

Ahrens, B., Braakhekke, M. C., Guggenberger, G., Schrumpf, M. and Reichstein, M.: Contribution of sorption, DOC transport and microbial interactions to the ^{14}C age of a soil organic carbon profile: Insights from a calibrated process model, Soil Biol. Biochem., 88, 390–402.

Albrecht, A. and Kandji, S. T.: Carbon sequestration in tropical agroforestry systems, Agric. Ecosyst. Environ., 99, 15–27, 2003.

Anderson, S. H., Udawatta, R. P., Seobi, T. and Garrett, H. E.: Soil water content and infiltration in agroforestry buffer strips, Agrofor. Syst., 75(1), 5–16, 2009.

Andrianarisoa, K., Dufour, L., Bienaime, S., Zeller, B. and Dupraz, C.: The introduction of hybrid walnut trees (*Juglans nigra* x *regia* cv. NG23) into cropland reduces soil mineral N content in autumn in southern France, Agrofor. Syst., 90(2), 193–205, 2016.

Baisden, W. T. and Parfitt, R. L.: Bomb ^{14}C enrichment indicates decadal C pool in deep soil?, Biogeochemistry, 85, 59–68, 2007.

Baisden, W. T., Amundson, R., Brenner, D. L., Cook, A. C., Kendall, C. and Harden, J. W.: A multiisotope C and N modeling analysis of soil organic matter turnover and transport as a function of soil depth in a California annual grassland soil chronosequence, Global Biogeochem. Cycles, 16(4), 82-1-82–26, 2002.

Balandier, P. and Dupraz, C.: Growth of widely spaced trees. A case study from young agroforestry plantations in France, Agrofor. Syst., 43, 151–167, 1999.

Balesdent, J., Mariotti, A. and Boisgontier, D.: Effect of tillage on soil organic carbon mineralization estimated from ^{13}C abundance in maize fields, J. Soil Sci., 41(4), 587–596, 1990.

Bambrick, A. D., Whalen, J. K., Bradley, R. L., Cogliastro, A., Gordon, A. M., Olivier, A. and Thevathasan, N. V: Spatial heterogeneity of soil organic carbon in tree-based intercropping systems in Quebec and Ontario, Canada, Agrofor. Syst., 79, 343–353, 2010.

Bengtson, P., Barker, J. and Grayston, S. J.: Evidence of a strong coupling between root exudation, C and N availability, and stimulated SOM decomposition caused by rhizosphere priming effects, Ecol. Evol., 2(8), 1843–1852, 2012.

Blagodatsky, S., Blagodatskaya, E., Yuyukina, T. and Kuzyakov, Y.: Model of apparent and real priming effects: Linking microbial activity with soil organic matter decomposition, Soil Biol. Biochem., 42(8), 1275–1283, 2010.

Braakhekke, M. C., Beer, C., Hoosbeek, M. R., Reichstein, M., Kruijt, B., Schrumpf, M. and Kabat, P.: SOMPROF: A vertically explicit soil organic matter model, Ecol. Modell., 222(10), 1712–1730, 2011.

Bruun, S., Christensen, B. T., Thomsen, I. K., Jensen, E. S. and Jensen, L. S.: Modeling vertical movement of organic matter in a soil incubated for 41 years with ^{14}C labeled straw, Soil Biol. Biochem., 39(1), 368–371, 2007.

Burgess, P. J., Incoll, L. D., Corry, D. T., Beaton, A. and Hart, B. J.: Poplar (*Populus* spp) growth and crop yields in a silvoarable experiment at three lowland sites in England, Agrofor. Syst., 63, 157–169, 2004.

Cardinael, R., Mao, Z., Prieto, I., Stokes, A., Dupraz, C., Kim, J. H. and Jourdan, C.: Competition with winter crops induces deeper rooting of walnut trees in a Mediterranean alley

cropping agroforestry system, Plant Soil, 391, 219–235, 2015a.

Cardinael, R., Chevallier, T., Barthès, B. G., Saby, N. P. A., Parent, T., Dupraz, C., Bernoux, M. and Chenu, C.: Impact of alley cropping agroforestry on stocks, forms and spatial distribution of soil organic carbon - A case study in a Mediterranean context, Geoderma, 259–260, 288–299, 2015b.

Cardinael, R., Eglin, T., Guenet, B., Neill, C., Houot, S. and Chenu, C.: Is priming effect a significant process for long-term SOC dynamics? Analysis of a 52-years old experiment, Biogeochemistry, 123, 203–219, 2015c.

Cardinael, R., Chevallier, T., Cambou, A., Béral, C., Barthès, B. G., Dupraz, C., Durand, C., Kouakoua, E. and Chenu, C.: Increased soil organic carbon stocks under agroforestry: A survey of six different sites in France, Agric. Ecosyst. Environ., 236, 243–255, 2017.

Carney, K. M., Hungate, B. A., Drake, B. G. and Megonigal, J. P.: Altered soil microbial community at elevated CO_2 leads to loss of soil carbon, PNAS, 104(12), 4990–4995, 2007.

Charbonnier, F., le Maire, G., Dreyer, E., Casanoves, F., Christina, M., Dauzat, J., Eitel, J. U. H., Vaast, P., Vierling, L. A. and Roupsard, O.: Competition for light in heterogeneous canopies: Application of MAESTRA to a coffee (*Coffea arabica* L.) agroforestry system, Agric. For. Meteorol., 181, 152–169, 2013.

Chaudhry, A. K., Khan, G. S., Siddiqui, M. T., Akhtar, M. and Aslam, Z.: Effect of arable crops on the growth of poplar (*Populus deltoides*) tree in agroforestry system, Pakistan J. Agric. Sci., 40, 82–85, 2003.

Chifflot, V., Bertoni, G., Cabanettes, A. and Gavaland, A.: Beneficial effects of intercropping on the growth and nitrogen status of young wild cherry and hybrid walnut trees, Agrofor. Syst., 66(1), 13–21, 2006.

Clinch, R. L., Thevathasan, N. V., Gordon, A. M., Volk, T. A. and Sidders, D.: Biophysical

1020 interactions in a short rotation willow intercropping system in southern Ontario, Canada, Agric.
1021 Ecosyst. Environ., 131(1–2), 61–69, 2009.

1022 Conant, R. T., Ryan, M. G., Ågren, G. I., Birge, H. E., Davidson, E. A., Eliasson, P. E., Evans,
1023 S. E., Frey, S. D., Giardina, C. P., Hopkins, F. M., Hyvönen, R., Kirschbaum, M. U. F.,
1024 Lavallee, J. M., Leifeld, J., Parton, W. J., Megan Steinweg, J., Wallenstein, M. D., Martin
1025 Wetterstedt, J. Å. and Bradford, M. A.: Temperature and soil organic matter decomposition
1026 rates - synthesis of current knowledge and a way forward, Glob. Chang. Biol., 17(11), 3392–
1027 3404, 2011.

1028 Cotrufo, M. F., Wallenstein, M. D., Boot, C. M., Denef, K. and Paul, E.: The Microbial
1029 Efficiency-Matrix Stabilization (MEMS) framework integrates plant litter decomposition with
1030 soil organic matter stabilization: do labile plant inputs form stable soil organic matter?, Glob.
1031 Chang. Biol., 19(4), 988–95, 2013.

1032 Davidson, E. A. and Janssens, I. A.: Temperature sensitivity of soil carbon decomposition and
1033 feedbacks to climate change, Nature, 440, 165–173, 2006.

1034 Dimassi, B., Cohan, J.-P., Labreuche, J. and Mary, B.: Changes in soil carbon and nitrogen
1035 following tillage conversion in a long-term experiment in Northern France, Agric. Ecosyst.
1036 Environ., 169, 12–20, 2013.

1037 Dubbert, M., Mosena, A., Piayda, A., Cuntz, M., Correia, A. C., Pereira, J. S. and Werner, C.:
1038 Influence of tree cover on herbaceous layer development and carbon and water fluxes in a
1039 Portuguese cork-oak woodland, Acta Oecologica, 59, 35–45, 2014.

1040 Dufour, L., Metay, A., Talbot, G. and Dupraz, C.: Assessing Light Competition for Cereal
1041 Production in Temperate Agroforestry Systems using Experimentation and Crop Modelling, J.
1042 Agron. Crop Sci., 199(3), 217–227, 2013.

1043 Dunbabin, V. M., Postma, J. A., Schnepf, A., Pagès, L., Javaux, M., Wu, L., Leitner, D., Chen,

Y. L., Rengel, Z. and Diggle, A. J.: Modelling root-soil interactions using three-dimensional models of root growth, architecture and function, Plant Soil, 372(1–2), 93–124, 2013.

Dupuy, L., Gregory, P. J. and Bengough, A. G.: Root growth models: Towards a new generation of continuous approaches, J. Exp. Bot., 61(8), 2131–2143, 2010.

Duursma, R. and Medlyn, B.: MAESPA: a model to study interactions between water limitation, environmental drivers and vegetation function at tree and stand levels, with an example application to [CO_2] × drought interactions, Geosci. Model Dev., 5, 919–940, 2012.

Eilers, K. G., Debenport, S., Anderson, S. and Fierer, N.: Digging deeper to find unique microbial communities: The strong effect of depth on the structure of bacterial and archaeal communities in soil, Soil Biol. Biochem., 50, 58–65, 2012.

Eissenstat, D. M. and Yanai, R. D.: The Ecology of Root Lifespan, Adv. Ecol. Res., 27, 1–60, 1997.

Ellert, B. H. and Bettany, J. R.: Calculation of organic matter and nutrients stored in soils under contrasting management regimes, Can. J. Soil Sci., 75, 529–538, 1995.

Elzein, A. and Balesdent, J.: Mechanistic simulation of vertical distribution of carbon concentrations and residence times in soils, Soil Sci. Soc. Am. J., 59, 1328–1335, 1995.

Fierer, N., Schimel, J. P. and Holden, P. A.: Variations in microbial community composition through two soil depth profiles, Soil Biol. Biochem., 35(1), 167–176, 2003.

Fontaine, S., Barot, S., Barré, P., Bdioui, N., Mary, B. and Rumpel, C.: Stability of organic carbon in deep soil layers controlled by fresh carbon supply, Nature, 450, 277–281, 2007.

Germon, A., Cardinael, R., Prieto, I., Mao, Z., Kim, J. H., Stokes, A., Dupraz, C., Laclau, J.-P. and Jourdan, C.: Unexpected phenology and lifespan of shallow and deep fine roots of walnut trees grown in a silvoarable Mediterranean agroforestry system, Plant Soil, 401, 409–426, 2016.

Graves, A. R., Burgess, P. J., Palma, J. H. N., Herzog, F., Moreno, G., Bertomeu, M., Dupraz,

C., Liagre, F., Keesman, K., van der Werf, W., de Nooy, a. K. and van den Briel, J. P.: Development and application of bio-economic modelling to compare silvoarable, arable, and forestry systems in three European countries, Ecol. Eng., 29(4), 434–449, 2007.

Graves, A. R., Burgess, P. J., Palma, J., Keesman, K. J., van der Werf, W., Dupraz, C., van Keulen, H., Herzog, F. and Mayus, M.: Implementation and calibration of the parameter-sparse Yield-SAFE model to predict production and land equivalent ratio in mixed tree and crop systems under two contrasting production situations in Europe, Ecol. Modell., 221, 1744–1756, 2010.

van Groenigen, K. J., Qi, X., Osenberg, C. W., Luo, Y. and Hungate, B. A.: Faster decomposition under increased atmospheric CO_2 limits soil carbon storage, Science., 344, 508–509, 2014.

Guenet, B., Eglin, T., Vasilyeva, N., Peylin, P., Ciais, P. and Chenu, C.: The relative importance of decomposition and transport mechanisms in accounting for soil organic carbon profiles, Biogeosciences, 10(4), 2379–2392, 2013.

Guenet, B., Moyano, F. E., Peylin, P., Ciais, P. and Janssens, I. A.: Towards a representation of priming on soil carbon decomposition in the global land biosphere model ORCHIDEE (version 1.9.5.2), Geosci. Model Dev., 9, 841–855, 2016.

Haile, S. G., Nair, V. D. and Nair, P. K. R.: Contribution of trees to carbon storage in soils of silvopastoral systems in Florida, USA, Glob. Chang. Biol., 16, 427–438, 2010.

Hendrick, R. L. and Pregitzer, K. S.: Temporal and depth-related patterns of fine root dynamics in northern hardwood forests, J. Ecol., 84, 167–176, 1996.

Howlett, D. S., Moreno, G., Mosquera Losada, M. R., Nair, P. K. R. and Nair, V. D.: Soil carbon storage as influenced by tree cover in the Dehesa cork oak silvopasture of central-western Spain, J. Environ. Monit., 13(7), 1897–904, 2011.

Ilstedt, U., Bargués Tobella, A., Bazié, H. R., Bayala, J., Verbeeten, E., Nyberg, G., Sanou, J., Benegas, L., Murdiyarso, D., Laudon, H., Sheil, D. and Malmer, A.: Intermediate tree cover can maximize groundwater recharge in the seasonally dry tropics, Sci. Rep., 6, 21930, 2016.

IUSS Working Group WRB: World Reference Base for Soil Resources 2006, first update 2007. World Soil Resources Reports No. 103. FAO, Rome., 2007.

Jobbagy, E. G. and Jackson, R. B.: The vertical distribution of soil organic carbon and its relation to climate and vegetation, Ecol. Appl., 10, 423–436, 2000.

Joslin, J. D., Gaudinski, J. B., Torn, M. S., Riley, W. J. and Hanson, P. J.: Fine-root turnover patterns and their relationship to root diameter and soil depth in a ^{14}C-labeled hardwood forest, New Phytol., 172, 523–535, 2006.

Kätterer, T., Bolinder, M. A., Andrén, O., Kirchmann, H. and Menichetti, L.: Roots contribute more to refractory soil organic matter than above-ground crop residues, as revealed by a long-term field experiment, Agric. Ecosyst. Environ., 141, 184–192, 2011.

Keiluweit, M., Bougoure, J. J., Nico, P. S., Pett-Ridge, J., Weber, P. K. and Kleber, M.: Mineral protection of soil carbon counteracted by root exudates, Nat. Clim. Chang., 5, 588–595, 2015.

Kim, D.-G., Kirschbaum, M. U. F. and Beedy, T. L.: Carbon sequestration and net emissions of CH_4 and N_2O under agroforestry: Synthesizing available data and suggestions for future studies, Agric. Ecosyst. Environ., 226, 65–78 , 2016.

Koarashi, J., Hockaday, W. C., Masiello, C. A. and Trumbore, S. E.: Dynamics of decadally cycling carbon in subsurface soils, J. Geophys. Res., 117, 1–13, 2012.

Koven, C. D., Riley, W. J., Subin, Z. M., Tang, J. Y., Torn, M. S., Collins, W. D., Bonan, G. B., Lawrence, D. M. and Swenson, S. C.: The effect of vertically resolved soil biogeochemistry and alternate soil C and N models on C dynamics of CLM4, Biogeosciences, 10(11), 7109–7131, 2013.

Lange, M., Eisenhauer, N., Sierra, C. A., Bessler, H., Engels, C., Griffiths, R. I., Mellado-Vázquez, P. G., Malik, A. A., Roy, J., Scheu, S., Steinbeiss, S., Thomson, B. C., Trumbore, S. E. and Gleixner, G.: Plant diversity increases soil microbial activity and soil carbon storage, Nat. Commun., 6, 6707, 2015.

Lavelle, P.: Faunal activities and soil processes: adaptative strategy that determine ecosystem function., 1997.

Li, F., Meng, P., Fu, D. and Wang, B.: Light distribution, photosynthetic rate and yield in a Paulownia-wheat intercropping system in China, Agrofor. Syst., 74(2), 163–172, 2008.

Lorenz, K. and Lal, R.: Soil organic carbon sequestration in agroforestry systems. A review, Agron. Sustain. Dev., 34, 443–454, 2014.

Luedeling, E., Smethurst, P. J., Baudron, F., Bayala, J., Huth, N. I., van Noordwijk, M., Ong, C. K., Mulia, R., Lusiana, B., Muthuri, C. and Sinclair, F. L.: Field-scale modeling of tree-crop interactions: Challenges and development needs, Agric. Syst., 142, 51–69, 2016.

Mead, R. and Willey, R. W.: The concept of a "land equivalent ratio" and advantages in yields from intercropping, Exp. Agric., 16(3), 217–228, 1980.

Moreno, G., Obrador, J. J., Cubera, E. and Dupraz, C.: Fine root distribution in Dehesas of central-western Spain, Plant Soil, 277(1–2), 153–162, 2005.

Moyano, F. E., Vasilyeva, N., Bouckaert, L., Cook, F., Craine, J., Curiel Yuste, J., Don, A., Epron, D., Formanek, P., Franzluebbers, A., Ilstedt, U., Kätterer, T., Orchard, V., Reichstein, M., Rey, A., Ruamps, L., Subke, J. A., Thomsen, I. K. and Chenu, C.: The moisture response of soil heterotrophic respiration: Interaction with soil properties, Biogeosciences, 9, 1173–1182, 2012.

Moyano, F. E., Manzoni, S. and Chenu, C.: Responses of soil heterotrophic respiration to moisture availability: An exploration of processes and models, Soil Biol. Biochem., 59, 72–85,

2013.

Mulia, R. and Dupraz, C.: Unusual fine root distributions of two deciduous tree species in southern France: What consequences for modelling of tree root dynamics?, Plant Soil, 281, 71–85, 2006.

Mulia, R., Dupraz, C. and van Noordwijk, M.: Reconciling root plasticity and architectural ground rules in tree root growth models with voxel automata, Plant Soil, 337(1–2), 77–92, 2010.

Nair, P. K.: An introduction to agroforestry, Kluwer Academic Publishers, Dordrecht, The Netherlands., 1993.

Nair, P. K. R.: Classification of agroforestry systems, Agrofor. Syst., 3(2), 97–128, 1985.

van Noordwijk, M. and Lusiana, B.: WaNuLCAS, a model of water, nutrient and light capture in agroforestry systems, Agrofor. Syst., 43, 217–242, 1999.

Odhiambo, H. O., Ong, C. K., Deans, J. D., Wilson, J., Khan, A. A. H. and Sprent, J. I.: Roots, soil water and crop yield: Tree crop interactions in a semi-arid agroforestry system in Kenya, Plant Soil, 235(2), 221–233, 2001.

Oelbermann, M. and Voroney, R. P.: And evaluation of the century model to predict soil organic carbon: examples from Costa Rica and Canada, Agrofor. Syst., 82, 37–50, 2011.

Oelbermann, M., Voroney, R. P. and Gordon, A. M.: Carbon sequestration in tropical and temperate agroforestry systems: a review with examples from Costa Rica and southern Canada, Agric. Ecosyst. Environ., 104, 359–377, 2004.

Oelbermann, M., Voroney, R. P., Thevathasan, N. V., Gordon, A. M., Kass, D. C. L. and Schlönvoigt, A. M.: Soil carbon dynamics and residue stabilization in a Costa Rican and southern Canadian alley cropping system, Agrofor. Syst., 68(1), 27–36, 2006.

Ong, C. K. and Leakey, R. R. B.: Why tree-crop interactions in agroforestry appear at odds with tree-grass interactions in tropical savannahs, Agrofor. Syst., 45(1–3), 109–129, 1999.

1164 Parton, W. J., Schimel, D. S., Cole, C. V and Ojima, D. S.: Analysis of factors controlling soil
1165 organic matter levels in great plains grasslands, Soil Sci. Soc. Am. J., 51, 1173–1179, 1987.

1166 Peichl, M., Thevathasan, N. V, Gordon, A. M., Huss, J. and Abohassan, R. A.: Carbon
1167 sequestration potentials in temperate tree-based intercropping systems, southern Ontario,
1168 Canada, Agrofor. Syst., 66, 243–257, 2006.

1169 Perveen, N., Barot, S., Alvarez, G., Klumpp, K., Martin, R., Rapaport, A., Herfurth, D.,
1170 Louault, F. and Fontaine, S.: Priming effect and microbial diversity in ecosystem functioning
1171 and response to global change: A modeling approach using the SYMPHONY model, Glob.
1172 Chang. Biol., 20(4), 1174–1190, 2014.

1173 Price, G. W. and Gordon, A. M.: Spatial and temporal distribution of earthworms in a temperate
1174 intercropping system in southern Ontario, Canada, Agrofor. Syst., 44, 141–149, 1999.

1175 Prieto, I., Roumet, C., Cardinael, R., Kim, J., Maeght, J.-L., Mao, Z., Portillo, N.,
1176 Thammahacksa, C., Dupraz, C., Jourdan, C., Pierret, A., Roupsard, O. and Stokes, A.: Root
1177 functional parameters along a land-use gradient: evidence of a community-level economics
1178 spectrum, J. Ecol., 103, 361–373, 2015.

1179 Prieto, I., Stokes, A. and Roumet, C.: Root functional parameters predict fine root
1180 decomposability at the community level, J. Ecol., 104, 725–733, 2016.

1181 R Development Core Team: R: A language and environment for statistical computing, 2013.

1182 Rasse, D. P., Mulder, J., Moni, C. and Chenu, C.: Carbon turnover kinetics with depth in a
1183 French loamy soil, Soil Sci. Soc. Am. J., 70, 2097–2105, 2006.

1184 Salomé, C., Nunan, N., Pouteau, V., Lerch, T. Z. and Chenu, C.: Carbon dynamics in topsoil
1185 and in subsoil may be controlled by different regulatory mechanisms, Glob. Chang. Biol., 16,
1186 416–426, 2010.

1187 Santaren, D., Peylin, P., Viovy, N. and Ciais, P.: Optimizing a process-based ecosystem model

with eddy-covariance flux measurements: A pine forest in southern France, Global Biogeochem. Cycles, 21, 1–15, 2007.

Schwarz, G.: Estimating dimension of a model, Ann. Stat., 6(2), 461–464, 1978.

Shahzad, T., Chenu, C., Genet, P., Barot, S., Perveen, N., Mougin, C. and Fontaine, S.: Contribution of exudates, arbuscular mycorrhizal fungi and litter depositions to the rhizosphere priming effect induced by grassland species, Soil Biol. Biochem., 80, 146–155, 2015.

Sierra, C. A., Trumbore, S. E., Davidson, E. A., Vicca, S. and Janssens, I.: Sensitivity of decomposition rates of soil organic matter with respect to simultaneous changes in temperature and moisture, J. Adv. Model. Earth Syst., 7, 335–356, 2015.

Soetaert, K., Petzoldt, T. and Woodrow Setzer, R.: Solving Differential Equations in R: Package deSolve, J. Stat. Softw., 33(9), 1–25, 2010.

Somarriba, E.: Revisiting the past: an essay on agroforestry definition, Agrofor. Syst., 19(3), 233–240, 1992.

Steinbeiss, S., Beßler, H., Engels, C., Temperton, V. M., Buchmann, N., Roscher, C., Kreutziger, Y., Baade, J., Habekost, M. and Gleixner, G.: Plant diversity positively affects short-term soil carbon storage in experimental grasslands, Glob. Chang. Biol., 14(12), 2937–2949, 2008.

Sulman, B. N., Phillips, R. P., Oishi, A. C., Shevliakova, E. and Pacala, S. W.: Microbe-driven turnover offsets mineral-mediated storage of soil carbon under elevated CO_2, Nat. Clim. Chang., 4, 1099–1102, 2014.

Taghizadeh-Toosi, A., Christensen, B. T., Hutchings, N. J., Vejlin, J., Kätterer, T., Glendining, M. and Olesen, J. E.: C-TOOL: A simple model for simulating whole-profile carbon storage in temperate agricultural soils, Ecol. Modell., 292, 11–25, 2014.

Talbot, G.: L'intégration spatiale et temporelle du partage des ressources dans un système

agroforestier noyers-céréales: une clef pour en comprendre la productivité ?, PhD Dissertation, Université Montpellier II., 2011.

Tarantola, A.: Inverse problem theory: methods for data fitting and model parameter estimation, edited by Elsevier., 1987.

Tarantola, A.: Inverse Problem Theory and Methods for Model Parameter Estimation, edited by SIAM., 2005.

Thevathasan, N. V. and Gordon, A. M.: Poplar leaf biomass distribution and nitrogen dynamics in a poplar-barley intercropped system in southern Ontario, Canada, Agrofor. Syst., 37, 79–90, 1997.

Udawatta, R. P., Kremer, R. J., Adamson, B. W. and Anderson, S. H.: Variations in soil aggregate stability and enzyme activities in a temperate agroforestry practice, Appl. Soil Ecol., 39(2), 153–160, 2008.

Virto, I., Barré, P., Burlot, A. and Chenu, C.: Carbon input differences as the main factor explaining the variability in soil organic C storage in no-tilled compared to inversion tilled agrosystems, Biogeochemistry, 108, 17–26, 2012.

van der Werf, W., Keesman, K., Burgess, P., Graves, A., Pilbeam, D., Incoll, L. D., Metselaar, K., Mayus, M., Stappers, R., van Keulen, H., Palma, J. and Dupraz, C.: Yield-SAFE: A parameter-sparse, process-based dynamic model for predicting resource capture, growth, and production in agroforestry systems, Ecol. Eng., 29(4), 419–433, 2007.

Wutzler, T. and Reichstein, M.: Colimitation of decomposition by substrate and decomposers - a comparison of model formulations, Biogeosciences, 5, 749–759, 2008.

Wutzler, T. and Reichstein, M.: Priming and substrate quality interactions in soil organic matter models, Biogeosciences, 10(3), 2089–2103, 2013.

Yin, R. and He, Q.: The spatial and temporal effects of paulownia intercropping: The case of

northern China, Agrofor. Syst., 37, 91–109, 1997.

Zhang, W., Wang, X. and Wang, S.: Addition of external organic carbon and native soil organic carbon decomposition: a meta-analysis., PLoS One, 8(2), e54779, 2013.